EUROPEAN COMMISSION

Community Research

SEVENTH FRAMEWORK PROGRAMME

ARCHER

Collaborative Project

Co-funded by the European Commission under the
Euratom Research and Training Programme on Nuclear Energy
within the Seventh Framework Programme

Grant Agreement Number: 269892
Start date: 01/02/2011 Duration: 48 Months

www.archer-project.eu

Archer
Advanced Reactor for Cogeneration of Heat & Electricity-R&D

Reports on graphite selection and recommended design properties.

Part I - results for the 750°C INNOGRAPH irradiation experiments (1A, 1B and 1C) Deliverable D41-16.

M W Davies (AMEC)

ARCHER project – Contract Number: 269892
Advanced High-Temperature Reactors for Cogeneration of Heat and Electricity R&D
EC Scientific Officer: Dr. Panagiotis Manolatos

Document title	Reports on graphite selection and recommended design properties. Part I - results for the 750°C INNOGRAPH irradiation experiments (1A, 1B and 1C).
Author(s)	M W Davies (AMEC)
Number of pages	47
Document type	Report
Work Package	WP41
Document number	D41-16
Issued by	AMEC
Date of completion	29/01/15
Dissemination level	Restricted to the partners of the ARCHER project

Summary

This document contains the assessment of the 750°C graphite irradiation experiments INNOGRAPH 1A, 1B and 1C. The assessment looks at the dimensional change behaviour of the graphites tested, along with the changes in dynamic Young's modulus, coefficient of thermal expansion and thermal conductivity. In terms of properties, the assessment shows that all the graphites behave qualitatively in the same way, and in a similar way to graphites irradiated in the past. However, there are significant differences in the dimensional change behaviour of the different graphites, which is the most important attribute from a core design point of view. There were large differences between the extruded graphites and the iso-moulded graphites. This was attributed to the difference in grain size rather than the manufacturing method. Extruded graphites generally have a medium grain size (3mm down to 0.5mm), whereas iso-moulded graphites generally have fine to super-fine grain size (0.1mm down to 5µm). There were also significant differences found between the with-grain (WG) and against-grain (AG) directions, which was not expected for some graphites.

In terms of dimensional change behaviour, the critical factors are the rate of initial shrinkage, the peak shrinkage (i.e. at turn-around), the fluence at which this occurs, and the fluence at which cross-over occurs, which is when the dimensions/volume return to their pre-irradiation values. For any particular graphite, this is considered to be the limiting fluence for the core as it is impractical to design a core structure which can accommodate significant, if any, nett growth. For the graphites tested, the fluence for cross-over ranges from 8.5 dpa to 13.0 dpa for the AG direction, and 14.5 dpa to 22.5 dpa for the WG direction.

Approval

Rev.	Short description	First author	WP Leader	Domain leader	Coordinator
0	First issue	**M W Davies (AMEC)**	**A Vreeling (NRG)**	**D Buckthorpe (AMEC)**	**S Knoll (NRG)**

Distribution list

Name	Organisation	Comments
P. Manolatos	EC DG RTD	
All technical participants	ARCHER	
Steering Committee members	ARCHER	

DOCUMENT ISSUE RECORD
(engineering documents)

Document Title :	**Reports on graphite selection and recommended design properties. Part I - results for the 750°C INNOGRAPH irradiation experiments (1A, 1B and 1C).**
Project Reference:	100525

Purpose of Issue : Issue to client

Security Class : Not protectively marked

Issue	Description of Amendment	Originator/ Author	Checker	Approver	Date
01	First Issue	M W Davies	D Buckthorpe	J O'Keefe	Jan 2015

Total number of pages:	Intro:		Text	46	Tables		Figures		Appendices	

Previous issues of this document shall be destroyed or marked **SUPERSEDED**

Distribution: ARCHER partners, M W Davies, D Buckthorpe, A Grainger

Table of contents

1 Introduction & Scope

In order to support the development of a future European High Temperature Reactor (HTR), a number of candidate graphites were selected for an irradiation programme. This programme was undertaken by NRG using the high flux reactor (HFR) at Petten and was aimed at establishing the irradiation behaviour of selected graphites over the fluence and temperature range appropriate for a HTR. This would allow the 'best' graphite(s) to be selected and would provide a significant amount of the data necessary to undertake a graphite core design.

Based on the reference design for the Pebble Bed Modular Reactor (PBMR) at the time, the peak fluence to be achieved for the irradiation programme was set at 25 displacements per atom (dpa), i.e. ~200 x 10^{20} n.cm^{-2} Equivalent DIDO Nickel Dose (EDND), and the temperature range was set at 550°C to 950°C. It was decided to carry out the first irradiation experiment at the mid-point of the temperature range i.e. 750°C, and to a maximum fluence of ~ 1/3 of the target peak fluence, i.e. 8-9 dpa (~65-70 x 10^{20} n.cm^{-2} EDND). This was referred to as INNOGRAPH 1A (Ref 1) and was carried out within the 5th Framework Programme (HTR-M1). A full post-irradiation examination (PIE) of the samples was carried out (Ref 2). This involved measuring their new dimensions and mass (from which their new volumes and densities were calculated) as well as dynamic Young's modulus (DYM), coefficient of thermal expansion (CTE) and thermal diffusivity (from which their thermal conductivity was calculated). The results were assessed in Ref 3.

The follow-up experiment at 750°C was planned to achieve a maximum fluence of ~2/3 of the target peak fluence, i.e..15-16 dpa (~125-130 x 10^{20} n.cm^{-2} EDND), This was referred to as INNOGRAPH 1B (Ref 4) and was carried out in the 6th Framework Programme (RAPHAEL). After the PIE of the INNOGRAPH 1A samples was carried out, around half of the samples were placed in the INNOGRAPH 1B experiment, the remaining positions being filled with fresh graphite specimens. With this arrangement, the fresh samples would see ~2/3 of the peak fluence and the samples previously irradiated in INNOGRAPH 1A would be irradiated up towards the peak fluence. Due to the flux buckling of the HFR, each experiment would see a range of fluences, with the samples at the top and bottom seeing about 0.65 of the fluence in the centre. Unfortunately, due to a lengthy unplanned shutdown of the HFR and the use of a lower enrichment fuel in the latter months, the target fluence for INNOGRAPH 1B was not achieved and so the overall (i.e. combined 1A and 1B) peak fluence of 25 dpa was not achieved. The maximum fluence for INNOGRAPH 1B was ~14 dpa, and so the peak fluence achieved by some of the INNOGRAPH 1A samples was ~23 dpa.

The full PIE of all the INNOGRAPH 1B specimens (Ref 5) was carried out as part of the 7th Framework Programme (ARCHER). In addition, another irradiation experiment was carried out in ARCHER at 750°C, but this time only to a fluence of ~1-2 dpa (~12-25 x 10^{20} n.cm^{-2} EDND). This was aimed at getting a better understanding of the variation in some properties that change rapidly over the first 1-2 dpa of irradiation. This was referred to as INNOGRAPH 1C (Ref 6) and the full PIE of the samples is reported in Ref 7. The assessment of all the INNOGRAPH 1A, 1B and 1C data, covering dimensional change, DYM, CTE and thermal conductivity, is the subject of this report, which is one of a series of three reports (see Note below).

[Note - Another two irradiation experiments, referred to as INNOGRAPH 2A and 2B, were also carried out in the 6th Framework Programme (RAPHAEL) These are the equivalent of INNOGRAPH 1A and 1B, but at a higher temperature of 950°C, and to a peak fluence of ~14 dpa (~120 x 10^{20} n.cm^{-2} EDND). The lower fluence was specified at the outset because the higher temperature would result in a lower fluence to dimensional change turnaround and to positive growth, which is a limiting feature of the capsule design. The PIE of all the specimens was also completed within ARCHER and the assessment of the data, including dimensional change, DYM, CTE and thermal conductivity is carried out in a companion to this report, Ref 8. Another companion report, Ref 9, looks at all the INNOGRAPH data. It recommends design properties and discusses graphite selection].

2 Graphite grades/samples

There is clearly a limit on the number of samples that can be contained within a given irradiation experiment, and as there is a need to maximise the number of samples of each graphite selected to provide good statistics, this had an influence on the number of graphites that can be tested. Another important consideration was that the general anisotropy of the different graphites requires samples to be machined from the two major directions, that is, 'with grain' (WG) and 'against grain' (AG). In addition, due to the

inherent material variability within a block, samples should be taken from both the centre region of a block and from the outside region of the block (hereafter referred to as 'centre' and 'edge' in this report).

After careful consideration of candidate graphites from 3 manufacturers (GraphTech, SGL and Toyo Tanso), 8 were chosen for INNOGRAPH 1A. Of these, 5 were classified as 'major' grades, the other 3 being classified as 'minor' grades. The intention was to cover the two main sources of coke (petroleum and pitch), and the two most common manufacturing techniques (extrusion and iso-moulding). Due to a decision to use a mixture of two sample lengths (6 mm and 12 mm) it was possible to maximise the number of samples that could be tested. Around 200 samples were included in INNOGRAPH 1A, with ~30 samples for each major grade and ~15 samples for each minor grade. The selected graphites (grouped in terms of manufacturer) are shown in Table 1 below.

Manufacturer	Grade	Coke	Process	Classification
GrafTech	PCEA	Petroleum	Extrusion	Major
	PPEA	Pitch	Extrusion	Minor
	PCIB-SFG	Petroleum	Iso-moulding	Major
SGL	NBG-10	Pitch	Extrusion	Major
	NBG-20*	Petroleum	Extrusion	Minor
	NBG-25	Petroleum	Iso-moulding	Major
Toyo Tanso	IG-110	Petroleum	Iso-moulding	Major
	IG-430	Pitch	Iso-moulding	Minor

Table 1 – Selected graphites for the INNOGRAPH 1A irradiation experiment

While this experiment was underway, another review of candidate graphites was made for INNOGRAPH 2A. It was decided to include another 3 candidate graphites in this experiment, making 11 in total. Two of these grades (NBG-18 and NBG-17) were manufactured by vibro-moulding, which is a more recent development, and were the selected graphites for the PBMR and ANTARES HTRs respectively. The third (LPEB/BAN) was found to exhibit the most isotropic dimensional change behaviour out of materials tested in the past. It was also decided to include the same 11 graphites in INNOGRAPH 1B, but in order to accommodate these, a few grades were interchanged between major and minor, and vice versa, a few were reduced from major to minor, and NBG-20 was removed. In addition, fewer 12 mm long samples were used. The selected graphites for INNOGRAPH 1B (grouped in terms of manufacturer) are shown in Table 2 below.

Manufacturer	Grade	Coke	Process	Classification
GrafTech	PCEA	Petroleum	Extrusion	Major
	PPEA	Pitch	Extrusion	Major
	PCIB-SFG	Petroleum	Iso-moulding	Minor
	LPEB/BAN	Petroleum	Extrusion	Minor
SGL	NBG-10	Pitch	Extrusion	Major
	NBG-25	Petroleum	Iso-moulding	Minor
	NBG-17	Pitch	Vibro-moulding	Minor
	NBG-18	Pitch	Vibro-moulding	Major
Toyo Tanso	IG-110	Petroleum	Iso-moulding	Minor
	IG-430	Pitch	Iso-moulding	Minor

Table 2 – Selected graphites for the INNOGRAPH 1B irradiation experiment

3 Pre-characterisation and post-irradiation measurements

3.1 Pre-characterisation measurements

The graphite blocks supplied by the manufacturers for each grade were sectioned and machined to produce the required number of samples. Each sample was cylindrically shaped with a nominal diameter of 8 mm and a nominal length of 6 or 12 mm. As mentioned earlier, the samples were machined from both the central and outer regions of each block, to take account of the known variability in properties throughout it. In addition, a small flat was also machined on each sample so that it could be uniquely identified with an alphanumeric code, and its orientation within the block would be known for recording the measurements (Figure 1). In this way, initial property variations as a function of position and orientation in the block could be determined (as well as for the irradiated properties).

The dimensions of each sample (see Section 3.2) were measured together with its DYM, CTE and thermal diffusivity (used to calculate thermal conductivity). The mass of each sample was also measured, which together with the dimensions, allowed the initial density to be determined. Details of the testing methods used are given in Ref 1. All the measurements (together with specific properties derived from them) were recorded in an Excel spreadsheet developed by NRG.

[Note - Although strength is a very important property from a core design point of view, it cannot be measured on the samples to be irradiated as this will involve a destructive test. Nevertheless, strength measurements can be made on other suitable samples obtained from a disc/block, and the strength distribution thus obtained should be representative of those being irradiated. Measurements of non-irradiated and irradiated strength were carried out within the ARCHER programme and the results are reported in Ref 10. All show the typical behaviour, which is an initial sharp increase at low fluence, followed by a plateau and then a further rise to a peak, after which it continues to fall.

3.2 Sample Orientations

Given the need to cover both principal directions (WG and AG), the cylindrical shape of the samples with the machined flat meant that great care had be used to ensure that the principal directions were maintained for each sample during manufacture. Figure 2 shows the orientations of the samples taken from both an extruded block and an iso-/vibro-moulded block. It can be seen that the extruded block has one principal WG direction and two principal AG directions, whereas the iso-/vibro-moulded block has two principal WG directions and one principal AG direction. The figure also shows the three dimensions measured, namely the axial length (L), the major diameter (D) and the smaller diameter perpendicular to the flat (X). The samples are classified as WG or AG according to the axial direction, hence the axial length L is always in this (assigned) orientation. The classification of the other two dimensions however depends on its orientation and also which type of block it came from. Table 3 below gives the appropriate classifications.

Process	**Sample orientation**	**Classification**		
		L	**D**	**X**
Extrusion	WG	WG	AG	AG
	AG	AG	AG*	WG*
Iso-moulding, Vibro-moulding	WG	WG	WG*	AG*
	AG	AG	WG	WG

Table 3 – Classification of sample dimensions with respect to sample orientation

* These classifications rely on the flat being machined with the sample in (or very close to) the correct orientation. If this was not the case for any sample, these particular measurements will not be 100% WG or AG, but will be somewhere in between, and this would reduce their usefulness.

3.3 Post-irradiation examination measurements

All the measurements carried out for the pre-characterisation are also required on the irradiated samples (i.e. dimensions, mass, DYM, CTE and thermal diffusivity). All PIE measurements (together with specific properties derived from them) have been added alongside the pre-characterisation measurements in the Excel spreadsheets developed by NRG.

3.4 Assessment spreadsheet

As stated earlier, the INNOGRAPH experiments were aimed at establishing the irradiation behaviour of selected graphites over the fluence and temperature range appropriate for a HTR. This would allow the 'best' graphite(s) to be selected and would provide a significant amount of the data necessary to undertake a graphite core design. To faciltate this, a spreadsheet was developed by AMEC which arranges all the data in a convenient way that enables the appropriate material property behaviour 'curves' to be produced for each. The pre-characterisation data for each graphite were simply copied from the NRG spreadsheet to the first part of the individual worksheet for each grade (Figure 3) and the PIE data were copied to the second part (Figure 4). The third part of the spreadsheet (Figure 5) calculates the changes in the property, either expressed as a percentage change (dimensions and volume), or a fractional change (DYM, CTE and thermal conductivity). The AMEC spreadsheets were used to produce plots of the changes to individual dimensions (L, D and x), volume, DYM, CTE and thermal conductivity in terms of the absolute values as well as the percentage changes or fractional changes. The plots illustrate the difference between the WG and AG behaviour (anisotropy) and the scatter in the behaviour. If needed, any differences between the 'centre' and 'edge' samples for each direction can be determined.

In Sections 4 to 7 of this report, the dimensional change behaviour and the variations in DYM, CTE and thermal conductivity are assessed for the 7 graphites that were in both INNOGRAPH 1A and 1B, namely NBG10, NBG25, PCEA, PPEA, PCIB, IG-110 and IG-430. All these graphites were irradiated to near full fluence. The graphites that were only in INNOGRAPH 1A or only in INNOGRAPH 1B, namely NBG20, NBG17, NBG18 and LPEB/BAN were only irradiated to either 1/3rd or 2/3rd of the full fluence respectively, and the sample data was limited. It was not possible to carry out a proper assessment of their behaviour over the full fluence range, and so these have not been included in this analysis. [Note – the 7 graphites that were in both INNOGRAPH 1A and 1B were also included in INNOGRAPH 1C and so it was possible to get a much better definition of the property variations at low fluences, particularly for those properties that vary rapidly at low fluence, namely DYM and thermal conductivity.

4 Dimensional change behaviour due to irradiation

The irradiation behaviour of the 7 INNOGRAPH 1A & 1B graphites in terms of the linear dimensional changes for the WG and AG directions, and the volumetric changes, are given in Figures 6 to 12. The plots are all shown over the same ranges (-4.0% to +8.0% for dimensional change and -10% to +20% for volumetric change) to give a direct visual comparison of the different behaviours. A negative value indicates shrinkage/volume reduction and a positive value indicates that there is a nett growth/volume increase relative to the unirradiated values. Fourth order equations (trendlines) generated by Excel have been fitted to the data where appropriate. (Fourth order equations give a better representation of the dimensional change behaviour at lower fluences than third order equations, and appear to confirm previous suggestions that the dimensional change and volume change rates at low fluences are much smaller than at higher fluences). The behaviour of each graphite is covered in Sub-sections 4.1 to 4.3 below in terms of manufacturer. A discussion on the specific differences and similarities between the behaviour of the different grades is given in Sub-section 4.4.

4.1 SGL grades

For NBG-10, which is a pitch coke extruded graphite, it can be seen from Figure 6a that there is some anisotropy with regard to dimensional change. The maximum average shrinkage is -1.9% (at 11.5 dpa) in the WG direction. This is larger than that for the AG direction, which is -1.4% (at 10.4 dpa). The larger shrinkage and later turnaround for the WG direction results in a slightly higher fluence to (average) cross-

over, being 18.7 dpa for the WG direction compared to 16.3 dpa for the AG direction. The delay also means that the maximum growth reached at the end of the experiment for the WG direction, at +2.1%, is less than that for the AG direction, at +3.9%. There is also quite a lot of scatter in the data at the higher fluences. The volume change behaviour is shown in Figure 6b. It can be seen that the maximum volume shrinkage is -4.7% (at 11.0 dpa). The average cross-over point occurs at 17.1 dpa and the average maximum volume growth at the peak fluence is +11.0%. The scatter for volume is clearly less than that for the dimensions up to the cross-over point, but thereafter it is broadly similar.

For NBG-25, which is a petroleum coke iso-moulded graphite, it can be seen from Figure 7a that there is a larger anisotropy with regard to dimensional change than for NBG-10, which would not be expected. The maximum average shrinkage is -1.9% (at 13.0 dpa) in the WG direction. This is much larger than that for the AG direction, which is only -0.6% (at 8.5 dpa). The larger shrinkage and much later turnaround for the WG direction results in a much higher fluence to (average) cross-over, being 20.0 dpa for the WG direction compared to only 13.0 dpa for the AG direction. The delay also means that the maximum growth reached at the end of the experiment for the WG direction, at +2.2%, is less than for the AG direction, at +5.4%. The volume change behaviour is shown in Figure 7b. It can be seen that the maximum volume shrinkage is -4.3% (at 12.0 dpa). The average cross-over point occurs at 18.3 dpa and the average maximum volume growth at the peak fluence is +10.0%. The scatter for volume is clearly less than that for the dimensions, but there are 3 clear 'outliers'. The scatter at higher fluence is less than that for NBG10.

4.2 GrafTech graphites

The GrafTech grades also cover both petroleum and pitch coke, and both extrusion and iso-moulding. For PCEA, which is a petroleum coke, extruded graphite, it can be seen from Figure 8a that there is some anisotropy with regard to dimensional change. The maximum average shrinkage is -2.7% (at 12.5 dpa) in the WG direction. This is larger than that for the AG direction, which is -2.0% (at 11.0 dpa). The larger shrinkage and later turnaround for the WG direction results in a higher fluence to (average) cross-over, being ~22.5 dpa for the WG direction compared to 18.2 dpa for the AG direction. The delay also means that the maximum dimensional change reached at the end of the experiment for the WG direction is much less than for the AG direction. For the former, the dimensions just reach their initial values, i.e. zero nett growth, whereas for the latter there is a growth of +2.5%. The volume change behaviour is shown in Figure 8b. It can be seen that the maximum volume shrinkage is -6.7% (at 11.5 dpa). The average cross-over point occurs at 19.1 dpa and the average maximum volume growth at the peak fluence is +5.0%. The scatter for volume is clearly less than that for the dimensions up to the cross-over point, but thereafter it is larger, but not as large as the scatter for dimensions.

For PPEA, which is the pitch-coke-equivalent of PCEA (and also the equivalent grade to NBG-10), it can be seen from Figure 9a that there is again some anisotropy The maximum average shrinkage in the WG direction is -2.0% (at 11.0 dpa). This is larger than in the AG direction, which is -1.4% (at 9.5 dpa). The larger shrinkage and later turnaround for the WG direction results in a higher fluence to (average) cross-over, being 18.9 dpa for the WG direction compared to 15.9 dpa for the AG direction. The delay also means that the maximum dimensional change reached at the end of the experiment for the WG direction is much less than for the AG direction. For the former, there is growth of +2.5%, whereas for the latter there is a growth of +5.0%. The volume change behaviour is shown in Figure 9b. It can be seen that the maximum volume shrinkage is -4.4% (at 10.5 dpa). The average cross-over point occurs at 16.9 dpa and the average maximum volume change at the peak fluence is +14%. The scatter is slightly less than for the individual dimensions.

For PCIB-SFG, which is a petroleum coke, iso-moulded super-fine-grain graphite, it can be seen from Figure 10a that there is again some anisotropy The maximum average shrinkage in the WG direction is -0.7% (at 8.5 dpa). This is larger than in the AG direction, which is -0.4% (at 6.0 dpa). The larger shrinkage and later turnaround for the WG direction results in a higher fluence to (average) cross-over, being 14.5 dpa for the WG direction compared to 11.0 dpa for the AG direction. The delay also means that the maximum dimensional change reached at the end of the experiment for the WG direction is much less than for the AG direction. For the former, there is growth of +3.4%, whereas for the latter there is a growth of +5.1%. The volume change behaviour is shown in Figure 10b. It can be seen that the maximum volume shrinkage is -1.8% (at 7.0 dpa). The average cross-over point occurs at 12.8 dpa and the average maximum volume

change at the peak fluence is +11.5%. The scatter is very small and slightly less than for the individual dimensions.

4.3 Toyo Tanso graphites

The Toyo Tanso grades cover both petroleum and pitch coke, but both are iso-moulded. For IG-110, which is the petroleum coke graphite, it can be seen from Figure 11a that there is again some anisotropy. The maximum average shrinkage in the WG direction is -1.9% (at 12.0 dpa). This is larger than in the AG direction, which is -1.2% (at 10.5 dpa). The larger shrinkage and later turnaround for the WG direction results in a higher fluence to (average) cross-over, being 19.2 dpa for the WG direction compared to 16.1 dpa for the AG direction. The delay also means that the maximum dimensional change reached at the end of the experiment for the WG direction is much less than for the AG direction. For the former, there is growth of +3.6%, whereas for the latter there is a growth of +6.6%. The volume change behaviour is shown in Figure 11b. It can be seen that the maximum volume shrinkage is -5.0% (at 11.0 dpa). The average cross-over point occurs at 18.2 dpa and the average maximum volume change at the peak fluence is +14.8%. The scatter is very small and slightly less than for the individual dimensions

For IG-430, which is the pitch coke equivalent of IG-110, it can be seen from Figure 12a that there is a very large anisotropy, which is not expected. The maximum average shrinkage in the WG direction is -1.3% (at 11.5 dpa). This is larger than in the AG direction, which is -0.4% (at 5.5 dpa). The larger shrinkage and later turnaround for the WG direction results in a higher fluence to (average) cross-over, being 17.2 dpa for the WG direction compared to 9.2 dpa for the AG direction. The delay also means that the maximum dimensional change reached at the end of the experiment for the WG direction is much less than for the AG direction. For the former, there is growth of +3.7%, whereas for the latter there is a growth of +8.0%. The volume change behaviour is shown in Figure 12b. It can be seen that the maximum volume shrinkage is -2.5% (at 10.0 dpa). The average cross-over point occurs at 15.0 dpa and the average maximum volume change at the peak fluence is +15.8%. The scatter is quite small and less than for the individual dimensions.

4.4 Discussion

It can be seen that all of graphites tested show the same qualitative dimensional change behaviour, but there is a significant difference in the quantitative behaviour between the different grades. Table 4 gives a summary of the important measures of dimensional change behaviour from a core design point of view, namely, the peak shrinkages reached at turn-around (for both WG and AG directions), the fluences at which these occur, and the fluences at which the original dimensions and volumes are reached (cross-over). The maximum dimensional and volume growths at the peak fluences attained are also given, although these are more of an academic interest as any realistic core designs will not be able to accommodate any significant growth, if any, and so the cross-over point would be the general fluence limit applied.

As a general observation, it can be seen that the AG direction for all the graphites exhibited less shrinkage than the WG grain direction. However, a consequence of this was that the AG direction always exhibited turn-around at a lower fluence than the WG direction and also reached cross-over at a lower fluence. For the AG direction, it can be seen from Table 4 that the maximum shrinkage attained was -2.0% (for PCEA), and this occurred at the highest fluence (11.0 dpa). This graphite also had the highest fluence to reach cross-over (18.2 dpa), which would be expected given it had the highest fluence to turn-around. The minimum shrinkage was -0.4% (for PCIB and IG-430) and these occurred at the lowest fluences (6.0 and 5.5 dpa respectively). These two graphites also had the lowest fluences to reach cross-over (11.0 and 9.2 dpa respectively), which again would be expected.

For the WG direction, it can be seen from Table 4 that the maximum shrinkage was again attained by PCEA (-2.7%), which occurred at the fluence of 12.5 dpa. This was not quite the highest fluence to turn-around which went to NBG-25 at 13.0 dpa. PCEA, however, still had the highest fluence to reach cross-over (22.5 dpa). The minimum WG shrinkage was -0.7% (for PCIB) which occurred at the lowest fluence (8.5 dpa). This graphite also had the lowest fluences to reach cross-over (14.5 dpa), which again would be expected.

Table 4 - Summary of dimensional and volume changes

Grade	Dimensional change - AG				Dimensional change - WG				Volume change			
	Maximum shrinkage	dpa to turn-around	dpa to cross-over	Maximum growth	Maximum shrinkage	dpa to turn-around	dpa to cross-over	Maximum growth	Maximum shrinkage	dpa to turn-around	dpa to cross-over	Maximum growth
NBG-10	-1.4	10.4	16.3	+3.9	-1.9	11.5	18.7	+2.1	-4.7	11.0	17.1	+11.0
PPEA	-1.4	9.5	15.9	+5.0	-2.0	11.0	18.9	+2.5	-4.4	10.5	16.9	+14.0
PCEA	-2.0	11.0	18.2	+2.5	-2.7	12.5	22.5	0.0	-6.7	11.5	19.1	+5.0
PCIB	-0.4	6.0	11.0	+5.1	-0.7	8.5	14.5	+3.4	-1.8	7.0	12.8	+11.5
NBG-25	-0.6	8.5	13.0	+5.4	-1.9	13.0	20.0	+2.2	-4.3	12.0	18.3	+10.0
IG-110	-1.2	10.5	16.1	+6.6	-1.9	12.0	19.2	+3.6	-5.1	11.5	18.2	+14.8
IG-430	-0.4	5.5	9.2	+8.0	-1.3	11.5	17.2	+3.7	-2.5	10.0	15.0	+15.8

In terms of volume change, it can be seen from Table 4 that the maximum volume shrinkage was again attained by PCEA (-6.7%), which occurred at a fluence of 11.5 dpa. This was not quite the highest fluence to volume turn-around which is at 12.0 dpa for NBG-25. PCEA, however, still has the highest fluence to reach volume cross-over (19.1 dpa). The minimum volume shrinkage was -1.8% (for PCIB) which occurred at the lowest fluence (7.0 dpa). This graphite also had the lowest fluences to reach cross-over (12.8 dpa), which again would be expected.

In terms of maximum growth and volume change, it can be seen from Table 4 that PCEA had the lowest maximum growth in the AG direction (+2.5%), and the WG direction (0.0%), and also volume change (+5.0%). In contrast, IG-430 had the highest maximum growth in the AG direction (+8.0%), and the WG direction (3.7%), and also volume change (+15.8%).

5 Dynamic Young's modulus

The variation in DYM with irradiation fluence for the 7 graphites is given in Figures 13 to 19. Figures 13a to 19a show the actual variations and Figures 13b to 19b show these as a fractional change, or multiplying factor (expressed as DYM_{irr}/DYM_{unirr}). All 7 graphites show the familiar trend seen for all graphites irradiated in the past. There is an initial very sharp increase in DYM over a fluence range of 0-1 dpa, and is represented by the black line. This is attributed to the pinning of mobile dislocations in the lattice structure. (In the UK this is referred to as the 'pinning' term). A short plateau is then reached, represented by the brown line, which continues up to around 5-6 dpa. At progressively higher fluences there is a further, but more gradual, increase in DYM attributed to structural changes within the crystals. (In the UK this is referred to as the 'structure' term). A peak value is then reached, and thereafter, the DYM decreases fairly rapidly thereafter as the graphite structure begins to break down.

Table 5 below summarises the initial DYM multiplying factor for each graphite along with the maximum multiplying factor and the approximate fluence at which this is reached. It can be seen that the DYM of all the extruded graphites have increased initially by a factor of around 1.45, whereas all the iso-moulded graphites have increased by a factor of between 1.60 and 1.69. The DYM of all the extruded graphites have increased by a factor of around 2.70 to 2.82 at the maximum fluence, whereas all the iso-moulded graphites have increased by a factor of between 3.15 and 3.48. The fluence at which the peak DYM is reached is fairly consistent across both graphite types, being between 14 and 16 dpa. (It should be noted that the strength of graphite also varies with fluence in a similar way to the DYM. Both multiplying factors, however, will be less than those for DYM).

Graphite	Type	Initial multiplying factor	Maximum multiplying factor	Fluence at which peak DYM is reached
NBG-10	Extruded	1.46	2.70	15
PPEA	Extruded	1.45	2.82	16
PCEA	Extruded	1.45	2.80	16
NBG-25	Iso-moulded	1.60	3.48	15
PCIB	Iso-moulded	1.60	3.28	16
IG-110	Iso-moulded	1.69	3.15	15
IG-430	Iso-moulded	1.60	3.24	14

Table 5 – Multiplying factors for the increases in DYM

6 Coefficient of thermal expansion

The variation in CTE with irradiation fluence for the 7 graphites is given in Figures 20 to 26. Figures 20a to 26a show the actual variations and Figures 20b to 26b show these as a fractional change, expressed as (CTE_{irr} / CTE_{unirr}) – 1, which is the customary way of doing this. Each plot shows the value of the mean CTE over 3 temperature ranges, 30-120°C, 30-200°C and 30-750°C. Most of the graphites show the familiar trend seen for all graphites irradiated in the past. There is a small initial increase in CTE over a fluence range of 0-2 dpa, after which there is a progressive decrease until a plateau is reached, and this plateau continues up to at least the peak fluence reached (~23 dpa). (This plateau is not however evident for IG-110 and IG-430 as no CTE measurements were made at the higher fluences).

7 Thermal conductivity

The variation in thermal conductivity with irradiation fluence for the 7 graphites is given in Figures 27 to 33. Figures 27a to 33a show the actual variations and Figures 27b to 33b show these as a fractional change, expressed as ($TCon_{irr}$ / $TCon_{unirr}$) – 1, which is the customary way of doing this. Each plot shows the value of the instantaneous thermal conductivity at temperatures of 27, 100, 200, 300, 400, 500, 600 and 700°C. It can be seen from Figures 27a to 33a that the unirradiated thermal conductivity of each graphite decreases with increasing temperature. When irradiated, all the graphites show the familiar trend seen for all graphites irradiated in the past. There is a very rapid decrease in thermal conductivity over a fluence range of 0-1 dpa, after which a plateau is reached. At higher fluences, a further decrease is observed, and this continued up until the peak fluence was reached. (This latter decrease cannot be seen for IG-110 and IG-430 as no thermal diffusivity measurements were made at the higher fluences).

It is interesting to note that, although there is a large spread in the unirradiated thermal conductivity over the measured temperature range (27° to 700°C), the variation is significantly reduced after a relatively small amount of irradiation. For example, Figure 27a shows that the spread in thermal conductivity for NBG-10 over the temperature range is ~160 W/m/K (at 27°C) to ~65 W/m/K at (700°C), a range of ~95 W/m/K. However, after only a few dpa of irradiation the thermal conductivity is ~40 W/m/K (at 27°C) to ~25 W/m/K at (700°C), a range of only ~15 W/m/K. At higher fluences, it can be seen that the range reduces further to ~10 W/m/K.

8 Conclusions

This document contains the assessment of the 750°C graphite irradiation experiments INNOGRAPH 1A, 1B and 1C. The assessment looks at the dimensional change behaviour of the graphites tested, along with the changes in DYM, CTE and thermal conductivity. In terms of properties, the assessment shows that all the graphites behave qualitatively in the same way, and in a similar way to graphites irradiated in the past. However, there are significant differences in the dimensional change behaviour of the different graphites, which is the most important attribute from a core design point of view. There were large differences between the extruded graphites and the iso-moulded graphites. This was attributed to the difference in grain size rather than the manufacturing method. Extruded graphites generally have a medium grain size (3mm down to 0.5mm), whereas iso-moulded graphites generally have fine to super-fine grain size (0.1mm down to 5µm). There were also significant differences found between the with-grain (WG) and against-grain (AG) directions, which was not expected for some graphites.

In terms of dimensional change behaviour, the critical factors are the rate of initial shrinkage, the peak shrinkage (i.e. at turn-around), the fluence at which this occurs, and the fluence at which cross-over occurs, which is when the dimensions/volume return to their pre-irradiation values. For any particular graphite, this is considered to be the limiting fluence for the core as it is impractical to design a core structure which can accommodate significant, if any, nett growth. The fluence for cross-over ranges from 8.5 dpa to 13.0 dpa for the AG direction, and 14.5 to 22.5 for the WG direction.

9 References

1 F. Schmalz et al., Preliminary irradiation testing of selected graphite grades for HTR, Final report on HTR-M1 WP3, 20787/05.71179/P, 19 December 2005

2 J.A. Vreeling, B. Sakintuna, DML3.13: Full PIE of INNOGRAPH-1A and description of INNOGRAPH-1B, NRG-21457/10.101850, 14 April 2010

3 M W Davies. Assessment of the full graphite irradiation results from INNOGRAPH 1A and comparison with previous data. RAPHAEL-1004-D-ML3.14

4 O. Wouters, J.A. Vreeling, INNOGRAPH-1B and INNOGRAPH-2A specimen manufacture and pre-characterisation, DML3.3: Graphite material procurement & characterisation, 21457/06.77300/P, 23 October 2006

5 M Heijna. High Dose. Experiments at 750℃ & 950℃ - Full PIE of INNOGRAPH-IB and INNOGRAPH-2B. ARCHER deliverable D41.12:

6 M Heijna. Final design proposal for the low dose irradiation experiment INNOGRAPH 1C. ARCHER deliverable D41-13

7 M Heijna. PIE report of low dose irradiation experiment at 750ºC, INNOGRAPH 1C. ARCHER deliverable D41-21

8 M W Davies. Reports on graphite selection and recommended design properties-Part II - results for the 950°C INNOGRAPH irradiation experiments (2A and 2B). ARCHER deliverable D41-17

9 M W Davies. Reports on graphite selection and recommended design properties-Part III – graphite selection and recommended design properties. ARCHER deliverable D41-18

10 M Heijna. Report on strength measurements of irradiated graphite. ARCHER deliverable D41-15

Figure 1 –

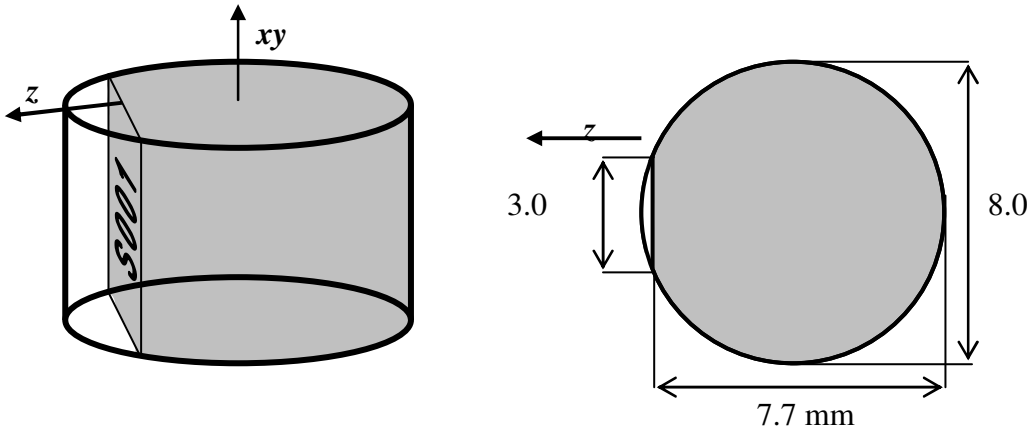

The figure on the left-hand side exaggeratedly shows the machined flat on the side of the cylinder. The milled plane is perpendicular to the *z*-direction when the axial direction of the cylinders in the *xy*-direction. The specimen number is engraved on the plane. The figure on the right-hand side is a top-view of the specimen. The important dimensions are indicated.

Figure 2

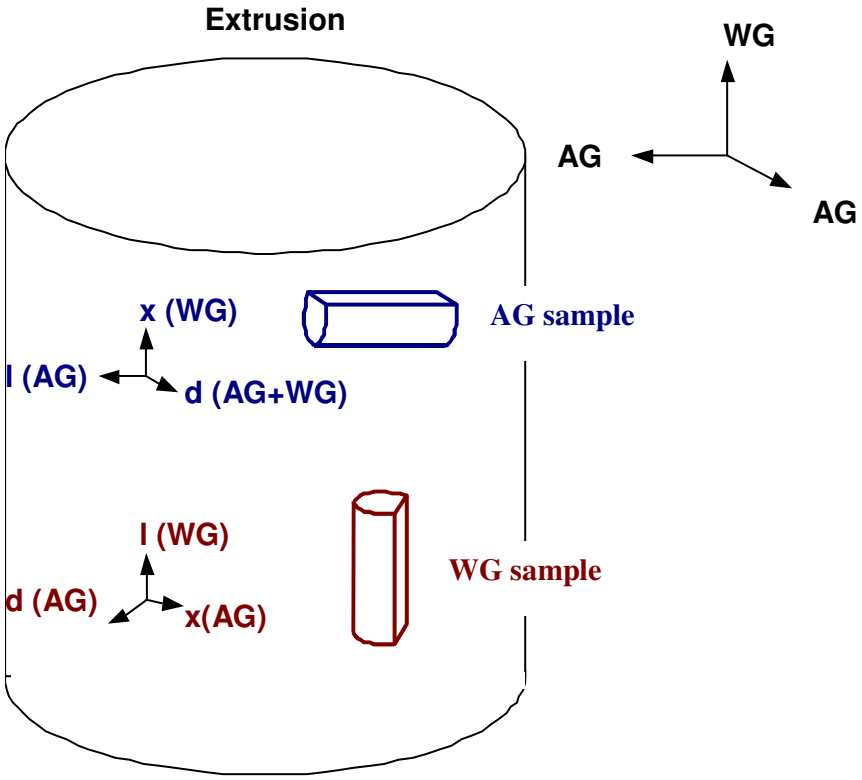

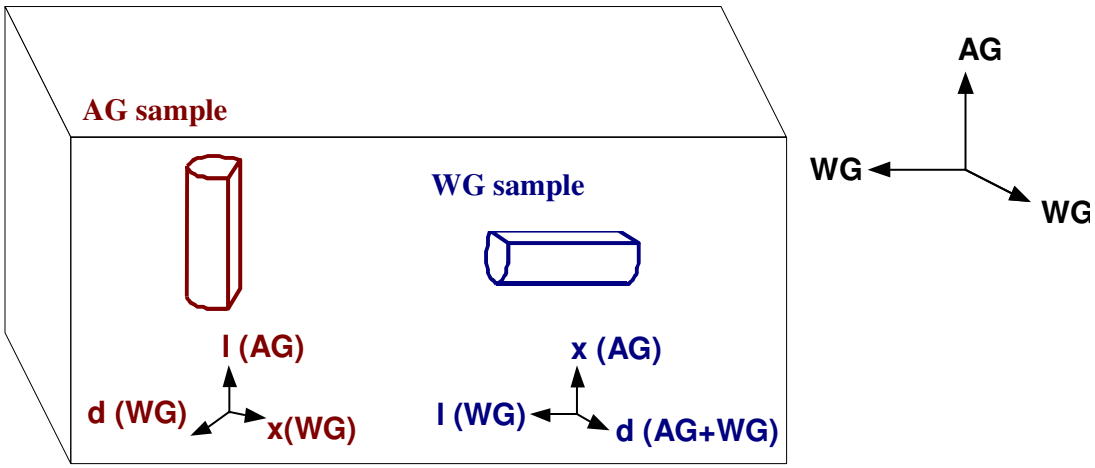

Iso-moulding

Figure 3 – Assessment spreadsheet – unirradiated values

Spec code	Block region	Orient-ation	Unirradiated properties																		
			Length L_o (mm)	Diam D_o (mm)	Diam x (mm)	Vol V_o (mm^3)	Mass Mo (g)	Density ρo (g/cm^3)	DYM E_o (GPa)	CTE α_o ($x10^{-6}$/K)			Thermal conductivity (W/m/K)							
										30-120	30-200	30-750	27°C	100°C	200°C	300°C	400°C	500°C	600°C	700°C
S024	CENTRE	WG	12.073	7.995	7.704	599.0	1.08118	1.805	13.3	4.19	4.38	5.25								
S028	CENTRE	WG	12.004	7.991	7.708	595.2	1.08534	1.823	13.5	4.07	4.24	5.24								
S029	CENTRE	WG	12.047	7.987	7.704	596.8	1.08031	1.810	12.7	4.26	4.46	5.32								
S030	CENTRE	WG	6.093	7.988	7.703	301.9	0.54858	1.817	13.7	4.07	4.24	5.24	141.8	132.3	116.8	102.4	93.1	86.1	77.2	70.6
S031	CENTRE	WG	6.047	7.994	7.707	300.0	0.54355	1.812	12.6	4.03	4.22	5.23	135.6	129.0	114.1	102.5	94.1	86.5	78.5	74.1
S032	CENTRE	WG	6.024	7.997	7.708	299.1	0.54231	1.813	13.3	4.09	4.26	5.25	141.9	130.7	115.2	101.6	93.9	85.8	77.8	71.7
S033	CENTRE	WG	6.025	7.994	7.704	298.9	0.54178	1.813	13.1	4.03	4.22	5.23	135.6	129.0	114.1	102.5	94.1	86.5	78.5	74.1
S034	CENTRE	WG	6.015	7.991	7.716	298.5	0.54019	1.810	12.8	4.11	4.29	5.26	142.0	129.1	113.6	100.7	94.8	85.5	78.5	72.7
S040	CENTRE	AG	6.079	7.987	7.705	301.2	0.54358	1.805	12.0	4.12	4.31	5.34	134.3	128.6	112.1	98.8	93.2	84.7	77.6	72.2
S041	CENTRE	AG	6.041	7.996	7.710	299.9	0.54485	1.817	12.6	4.12	4.31	5.34	134.3	128.6	112.1	98.8	93.2	84.7	77.6	72.2
S042	CENTRE	AG	6.084	7.969	7.698	300.2	0.54255	1.807	12.3	4.19	4.38	5.32	137.4	128.6	114.6	101.6	93.2	83.9	77.6	72.3
S043	CENTRE	AG	5.945	7.996	7.709	295.1	0.53777	1.822	12.5	4.19	4.38	5.32	137.4	128.6	114.6	101.6	93.2	83.9	77.6	72.3
S044	CENTRE	AG	6.103	7.981	7.704	302.0	0.54839	1.816	12.7	4.02	4.29	5.28	135.0	128.0	114.7	103.1	91.7	85.4	78.7	72.6
S050	CENTRE	AG	6.102	7.967	7.705	301.2	0.54449	1.808	12.3	4.20	4.39	5.40	137.4	128.6	114.6	101.6	93.2	83.9	77.6	72.3
S052	CENTRE	AG	6.057	7.981	7.704	299.7	0.54155	1.807	12.2	4.18	4.39	5.37	137.4	128.6	114.6	101.6	93.2	83.9	77.6	72.3
S054	CENTRE	AG	11.985	7.985	7.782	596.0	1.07834	1.809	12.5	3.96	4.32	5.36								
S055	CENTRE	AG	11.965	7.983	7.779	594.7	1.07937	1.815	12.7	3.96	4.32	5.36								
S200	CENTRE	AG	11.990	7.976	7.706	592.8	1.07194	1.808	13.0	4.12	4.42	5.37								
S057	EDGE	WG	12.075	8.018	7.709	601.9	1.09274	1.815	13.5	4.18	4.34	5.26								
S061	EDGE	WG	12.048	7.984	7.704	596.6	1.08662	1.821	13.5	4.18	4.34	5.26								
S063	EDGE	WG	6.105	7.980	7.699	301.9	0.54885	1.818	13.4	4.03	4.25	5.27	141.1	131.3	116.7	101.0	95.4	87.6	78.9	74.1
S065	EDGE	WG	5.864	7.977	7.696	289.8	0.52910	1.826	13.2	4.03	4.25	5.27	141.1	131.3	116.7	101.0	95.4	87.6	78.9	74.1
S067	EDGE	WG	6.119	7.991	7.695	303.2	0.54780	1.807	13.5	4.06	4.27	5.26	140.7	130.0	116.5	101.5	95.2	87.1	78.7	73.7
S069	EDGE	WG	6.031	7.992	7.704	299.0	0.54462	1.821	13.2	4.09	4.29	5.25	140.3	128.8	116.4	102.0	95.0	86.7	78.6	73.3
S071	EDGE	WG	6.026	7.995	7.704	299.0	0.54213	1.813	13.5	4.09	4.29	5.25	140.3	128.8	116.4	102.0	95.0	86.7	78.6	73.3
S072	EDGE	AG	6.113	7.987	7.711	303.0	0.55324	1.826	12.5	4.23	4.44	5.41	135.9	123.2	109.0	98.8	91.9	83.2	76.8	71.8
S073	EDGE	AG	6.080	7.996	7.710	301.8	0.54383	1.802	12.5	4.23	4.44	5.41	135.9	123.2	109.0	98.8	91.9	83.2	76.8	71.8
S074	EDGE	AG	6.115	7.983	7.704	302.7	0.55332	1.828	12.6	4.30	4.50	5.45	136.2	124.8	113.9	99.9	92.4	83.6	76.8	70.2
S076	EDGE	AG	5.985	7.977	7.703	295.9	0.53890	1.821	12.8	4.64	4.85	5.60	138.0	133.1	124.1	108.0	96.3	86.7	77.7	71.3
S084	EDGE	AG	11.964	7.984	7.781	594.9	1.08529	1.824	12.8	4.14	4.37	5.26								

Figure 4 – Assessment spreadsheet – irradiated values

Irrad temp (°C)	Fluence		Irradiated properties																
	DPA	EDND (10E22)	Length L_i (mm)	Diam D_i (mm)	Diam x_i (mm)	Vol V_i (mm^3)	Mass M_i (g)	Density ρ_i (g/cm^3)	DYM E_i (GPa)	CTE α_i ($x10^{-6}$/K)			Thermal conductivity (W/m/K)							
										30-120	30-200	30-750	27°C	100°C	200°C	300°C	400°C	500°C	600°C	700°C
750	9.54	72.5	11.827	7.890	7.604	571.553	1.080	1.889	27.932	1.72	1.91	3.10								
750	6.02	45.8	11.896	7.941	7.656	582.519	1.085	1.862	20.645	3.91	4.03	4.96								
750	8.76	66.6	11.802	7.888	7.605	570.142	1.079	1.893	29.379	2.06	2.16	3.13								
750	8.37	63.6	5.974	7.884	7.606	288.399	0.548	1.900	29.649	1.88	2.03	3.21	29.5	33.3	36.0	37.0	38.2	38.4	38.1	37.4
750	6.80	51.7	5.968	7.924	7.606	290.366	0.542	1.868	23.224	1.81	2.10	3.43	30.1	33.8	36.3	37.2	38.8	38.5	38.0	37.4
750	6.75	51.3	5.954	7.932	7.662	291.104	0.542	1.861	20.781	3.52	3.68	4.71	31.3	36.4	38.4	39.4	40.3	40.8	40.5	39.4
750	9.03	68.6	5.908	7.886	7.601	285.266	0.541	1.898	26.593	1.95	2.14	3.37	31.3	35.1	38.3	39.3	40.2	40.4	39.5	38.6
750	7.12	54.1	5.946	7.921	7.646	289.781	0.539	1.862	21.067	2.87	3.12	4.28	32.1	35.1	38.0	39.1	39.9	40.4	39.6	39.0
750	7.00	53.2	6.004	7.903	7.608	290.976	0.543	1.865	22.582	2.10	2.39	3.59	28.9	32.3	34.7	35.1	37.2	37.9	37.3	37.5
750	9.06	68.9	5.945	7.881	7.581	286.382	0.545	1.902	26.160	2.15	2.33	3.53	31.2	34.9	37.6	38.2	39.7	39.8	39.6	38.7
750	9.12	69.3	5.994	7.853	7.568	286.932	0.542	1.889	26.918	1.91	2.07	3.35	31.5	34.3	37.5	38.1	39.7	39.1	39.0	38.3
750	8.34	63.4	5.852	7.885	7.579	282.080	0.537	1.905	27.967	1.72	1.99	3.31	28.9	31.8	34.9	36.1	37.8	38.2	37.5	37.3
750	6.97	53.0	6.041	7.912	7.619	293.451	0.548	1.866	20.328	3.29	3.40	4.36	32.5	34.9	37.7	38.6	39.2	40.5	39.6	39.3
750	6.51	49.5	6.033	7.898	7.621	292.321	0.543	1.858	20.769	2.57	2.78	3.92	28.3	32.6	35.0	36.1	37.4	37.8	36.5	36.6
750	7.36	55.9	5.980	7.884	7.598	288.505	0.541	1.874	22.231	2.47	2.71	3.95	31.9	35.6	38.3	38.8	40.0	40.3	39.7	38.7
750	9.02	68.6	11.793	7.872	7.642	569.110	1.078	1.894	25.944	2.45	2.50	3.63								
750	9.39	71.4	11.791	7.864	7.628	567.704	1.079	1.901	25.860	2.14	2.30	3.46								
750	7.37	56.0	11.847	7.891	7.606	572.710	1.072	1.871	20.383	3.03	3.19	4.24								
750	6.53	49.6	11.893	7.939	7.638	581.437	1.092	1.878	22.568	2.73	2.89	3.89								
750	9.15	69.5	11.808	7.876	7.615	569.523	1.086	1.907	28.924	1.93	2.03	3.15								
750	7.65	58.1	6.008	7.891	7.622	290.723	0.548	1.887	24.683	2.13	2.38	3.66	30.1	33.6	35.5	37.0	38.6	38.5	38.6	37.7
750	9.15	69.5	5.750	7.874	7.606	277.080	0.528	1.906	31.213	1.58	1.82	3.14	29.0	33.7	36.8	38.4	39.8	39.4	39.1	38.6
750	8.51	64.7	5.998	7.886	7.605	289.681	0.548	1.891	26.933	2.08	2.24	3.45	33.4	38.0	41.0	41.8	42.9	42.5	41.5	40.4
750	8.46	64.3	5.932	7.901	7.619	287.542	0.544	1.891	25.461	2.00	2.17	3.41	31.7	35.0	37.6	38.0	39.6	40.2	39.1	38.6
750	5.93	45.1	5.928	7.932	7.648	289.568	0.541	1.870	24.086	1.99	2.32	3.50	30.1	34.2	36.6	37.1	39.1	39.7	39.1	38.5
750	7.78	59.1	6.045	7.890	7.605	292.180	0.553	1.891	23.122	2.51	2.74	3.96	27.6	31.7	33.9	34.7	36.0	36.5	36.3	35.5
750	9.13	69.4	6.000	7.875	7.581	288.730	0.543	1.882	28.188	2.04	2.20	3.31	29.9	32.8	36.1	36.8	37.4	37.6	37.0	36.6
750	8.07	61.3	6.038	7.880	7.594	291.088	0.552	1.897	23.994	2.31	2.46	3.67	34.1	36.2	38.3	40.2	41.1	41.4	41.2	40.4
750	7.57	57.5	5.919	7.877	7.592	285.099	0.539	1.890	23.496	2.23	2.49	3.80	33.0	36.0	38.8	39.4	40.2	40.8	40.5	39.6
750	9.16	69.6	11.803	7.858	7.633	567.814	1.085	1.910	27.908	2.12	2.21	3.33								

Figure 5 – Assessment spreadsheet – %/fractional changes

Location	Orientation	Fluence		Fractional change																			
		DPA	EDND (10E22)	Length L (%)	Diam D (%)	Diam x (%)	Vol V (%)	Mass M	Density ρ	DYM E (Gpa)	CTE 30-120	CTE 30-200	CTE 30-750	Thermal conductivity 27°C	100°C	200°C	300°C	400°C	500°C	600°C	700°C		
CENT	WG	9.54	72.5	-2.0339	-1.3105	-1.3006	-4.5804	-0.0012	0.04673	2.09575	-0.589	-0.564	-0.410										
CENT	WG	6.02	45.8	-0.8943	-0.6153	-0.6733	-2.1364	-0.0007	0.02108	1.5248	-0.039	-0.049	-0.052										
CENT	WG	8.76	66.6	-2.0376	-1.2397	-1.2838	-4.471	-0.0012	0.04555	2.30891	-0.517	-0.515	-0.411										
CENT	WG	8.37	63.6	-1.9606	-1.3069	-1.2571	-4.4842	-0.0012	0.04571	2.16044	-0.538	-0.520	-0.386	-0.792	-0.748	-0.691	-0.638	-0.590	-0.554	-0.506	-0.470		
CENT	WG	6.80	51.7	-1.3152	-0.8664	-1.3028	-3.2204	-0.0021	0.03108	1.83882	-0.550	-0.502	-0.344	-0.778	-0.738	-0.682	-0.637	-0.588	-0.555	-0.516	-0.495		
CENT	WG	6.75	51.3	-1.162	-0.8122	-0.5989	-2.6655	-0.0009	0.02641	1.56628	-0.139	-0.135	-0.102	-0.779	-0.722	-0.666	-0.612	-0.571	-0.524	-0.480	-0.451		
CENT	WG	9.03	68.6	-1.9356	-1.3515	-1.3395	-4.563	-0.0006	0.04722	2.03259	-0.516	-0.491	-0.356	-0.769	-0.728	-0.665	-0.617	-0.572	-0.533	-0.497	-0.479		
CENT	WG	7.12	54.1	-1.1521	-0.8835	-0.9163	-2.9056	-0.0014	0.02852	1.64829	-0.302	-0.273	-0.185	-0.774	-0.728	-0.665	-0.612	-0.579	-0.528	-0.496	-0.464		
CENT	AG	7.00	53.2	-1.2308	-1.0455	-1.2619	-3.3836	-0.0018	0.03313	1.88694	-0.490	-0.445	-0.328	-0.785	-0.748	-0.690	-0.645	-0.601	-0.552	-0.518	-0.481		
CENT	AG	9.06	68.9	-1.5815	-1.4404	-1.6633	-4.4975	-0.0002	0.04688	2.07311	-0.478	-0.459	-0.339	-0.768	-0.729	-0.665	-0.613	-0.574	-0.530	-0.489	-0.463		
CENT	AG	9.12	69.3	-1.4799	-1.451	-1.6866	-4.4229	-0.001	0.0452	2.18595	-0.545	-0.526	-0.370	-0.771	-0.733	-0.673	-0.625	-0.574	-0.534	-0.497	-0.470		
CENT	AG	8.34	63.4	-1.5611	-1.388	-1.6928	-4.4141	-0.0008	0.0453	2.23344	-0.589	-0.546	-0.377	-0.790	-0.753	-0.695	-0.645	-0.594	-0.545	-0.516	-0.485		
CENT	AG	6.97	53.0	-1.0113	-0.8706	-1.1008	-2.8318	-0.0016	0.02754	1.60173	-0.180	-0.208	-0.173	-0.759	-0.727	-0.671	-0.626	-0.572	-0.526	-0.497	-0.459		
CENT	AG	6.51	49.5	-1.1318	-0.8682	-1.0919	-2.9382	-0.0023	0.02796	1.68815	-0.388	-0.368	-0.274	-0.794	-0.746	-0.695	-0.645	-0.599	-0.550	-0.529	-0.495		
CENT	AG	7.36	55.9	-1.2675	-1.2191	-1.3772	-3.7311	-0.0018	0.0369	1.81754	-0.410	-0.382	-0.265	-0.768	-0.724	-0.666	-0.618	-0.570	-0.519	-0.488	-0.465		
CENT	AG	9.02	68.6	-1.6022	-1.4157	-1.7901	-4.5166	-0.0006	0.04663	2.07004	-0.382	-0.420	-0.322										
CENT	AG	9.39	71.4	-1.4548	-1.4889	-1.9385	-4.5465	-0.0003	0.04726	2.04141	-0.460	-0.467	-0.354										
CENT	AG	7.37	56.0	-1.1918	-1.0695	-1.2984	-3.3963	-0.0004	0.03477	1.56449	-0.266	-0.278	-0.210										
EDGE	WG	6.53	49.6	-1.5034	-0.9795	-0.9279	-3.3996	-0.0007	0.03446	1.67034	-0.348	-0.335	-0.260										
EDGE	WG	9.15	69.5	-1.9912	-1.3529	-1.1445	-4.5343	-0.0007	0.04673	2.14747	-0.538	-0.533	-0.402										
EDGE	WG	7.65	58.1	-1.5838	-1.1134	-0.9945	-3.7105	-0.0006	0.03786	1.84022	-0.473	-0.439	-0.305	-0.787	-0.744	-0.695	-0.634	-0.595	-0.561	-0.511	-0.492		
EDGE	WG	9.15	69.5	-1.9345	-1.2833	-1.163	-4.3825	-0.0018	0.04391	2.37356	-0.608	-0.571	-0.404	-0.794	-0.743	-0.685	-0.620	-0.583	-0.550	-0.504	-0.479		
EDGE	WG	8.51	64.7	-1.9777	-1.3078	-1.1657	-4.4609	-5E-05	0.04664	2.00168	-0.488	-0.476	-0.345	-0.763	-0.708	-0.648	-0.588	-0.549	-0.513	-0.473	-0.451		
EDGE	WG	8.46	64.3	-1.6402	-1.133	-1.1054	-3.844	-0.0017	0.03823	1.92863	-0.509	-0.494	-0.350	-0.774	-0.728	-0.677	-0.627	-0.584	-0.536	-0.503	-0.474		
EDGE	WG	5.93	45.1	-1.6309	-0.7932	-0.7317	-3.1574	-0.0012	0.03135	1.77944	-0.513	-0.460	-0.333	-0.786	-0.734	-0.685	-0.636	-0.589	-0.541	-0.502	-0.474		
EDGE	AG	7.78	59.1	-1.1099	-1.2084	-1.3661	-3.5561	-0.0012	0.03568	1.84878	-0.407	-0.383	-0.267	-0.797	-0.742	-0.688	-0.649	-0.608	-0.561	-0.527	-0.506		
EDGE	AG	9.13	69.4	-1.3044	-1.5087	-1.6771	-4.3363	-0.0007	0.04455	2.25428	-0.517	-0.504	-0.389	-0.780	-0.734	-0.669	-0.628	-0.594	-0.548	-0.518	-0.491		
EDGE	AG	8.07	61.3	-1.2462	-1.2909	-1.4235	-3.8388	-0.0018	0.03807	1.9074	-0.463	-0.453	-0.327	-0.750	-0.710	-0.664	-0.598	-0.555	-0.505	-0.464	-0.424		
EDGE	AG	7.57	57.5	-1.115	-1.2519	-1.4346	-3.6571	-0.0002	0.03777	1.82944	-0.520	-0.486	-0.321	-0.761	-0.729	-0.687	-0.635	-0.582	-0.529	-0.479	-0.444		
EDGE	AG	9.16	69.6	-1.3468	-1.5776	-1.8919	-4.5586	-0.0006	0.04711	2.18565	-0.487	-0.494	-0.366										

Figure 6 - Dimensional change and volume change for NBG-10

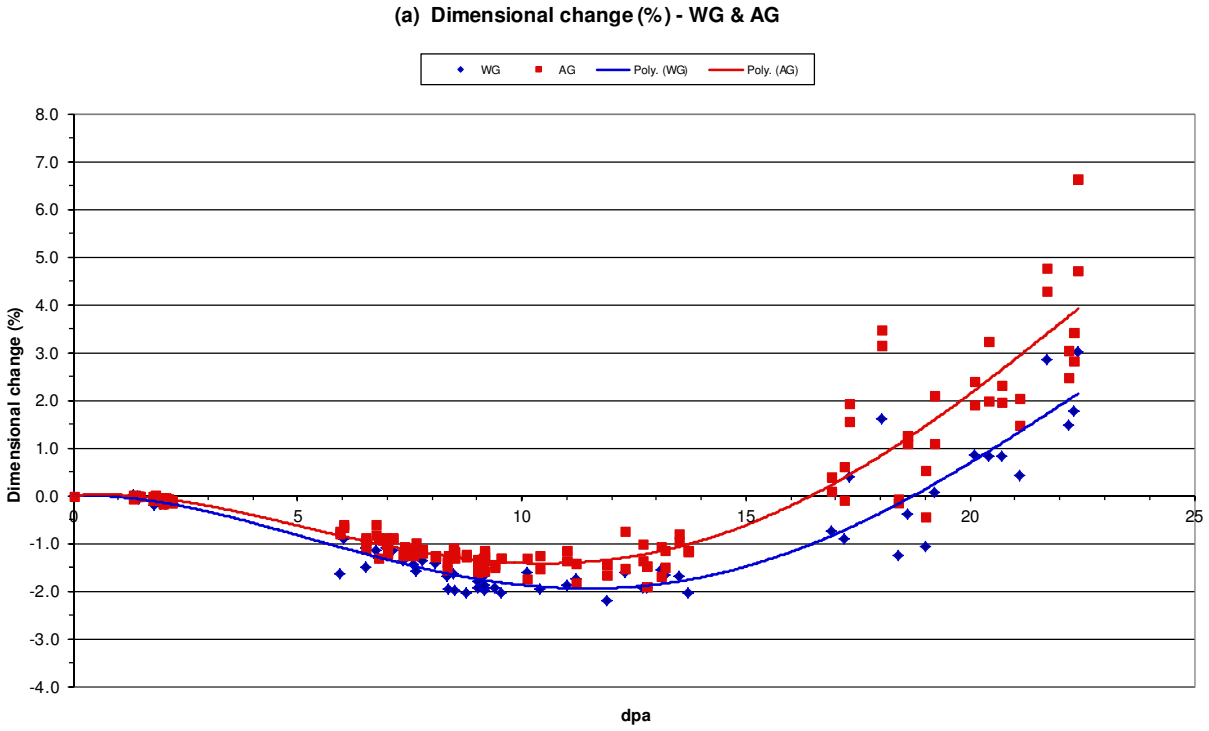

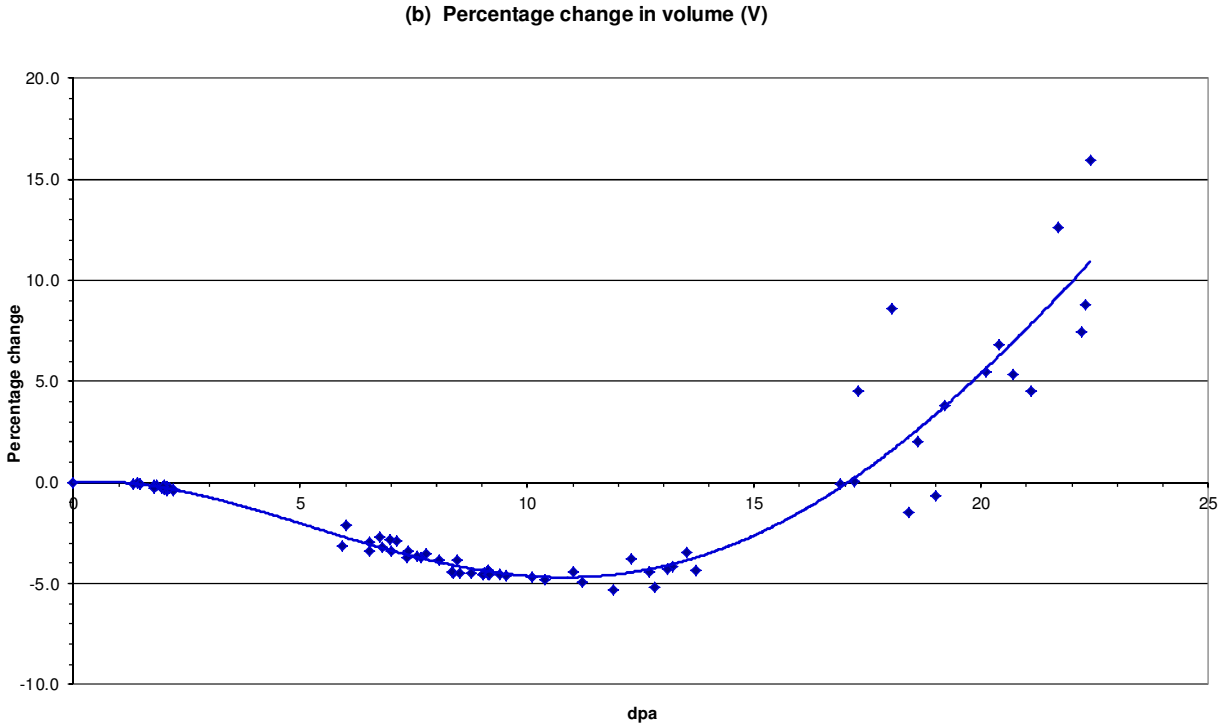

Figure 7 - Dimensional change and volume change for NBG-25

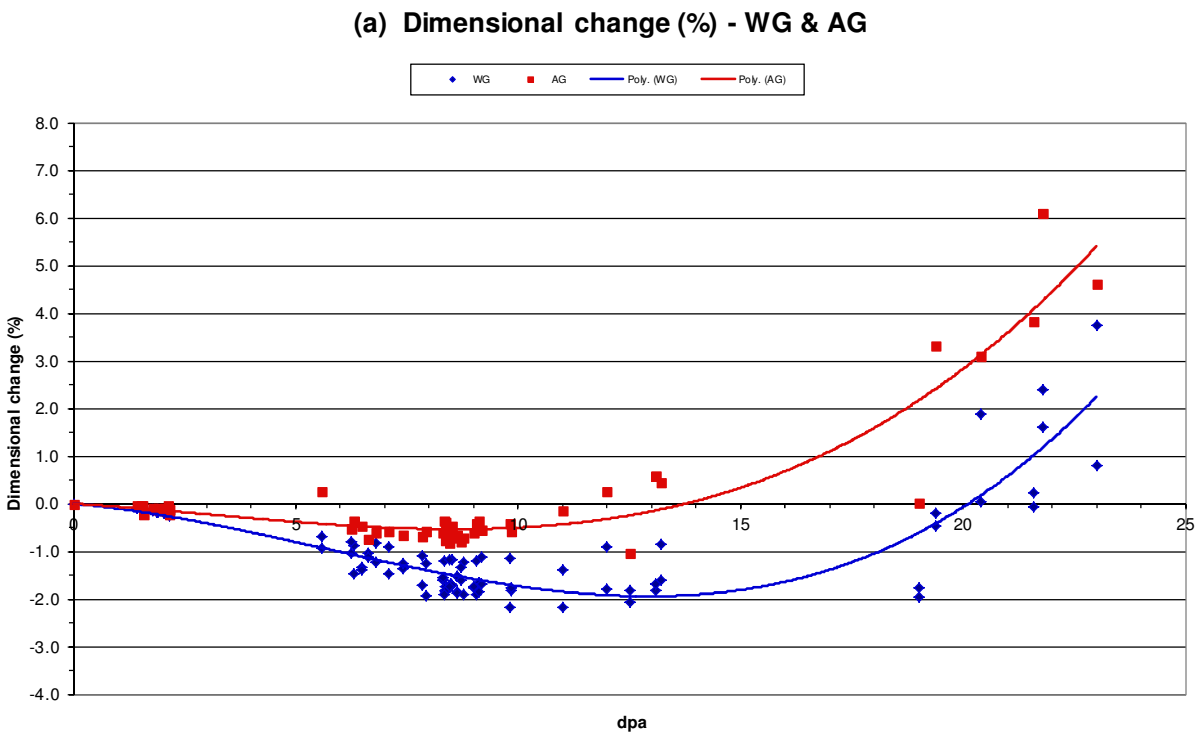

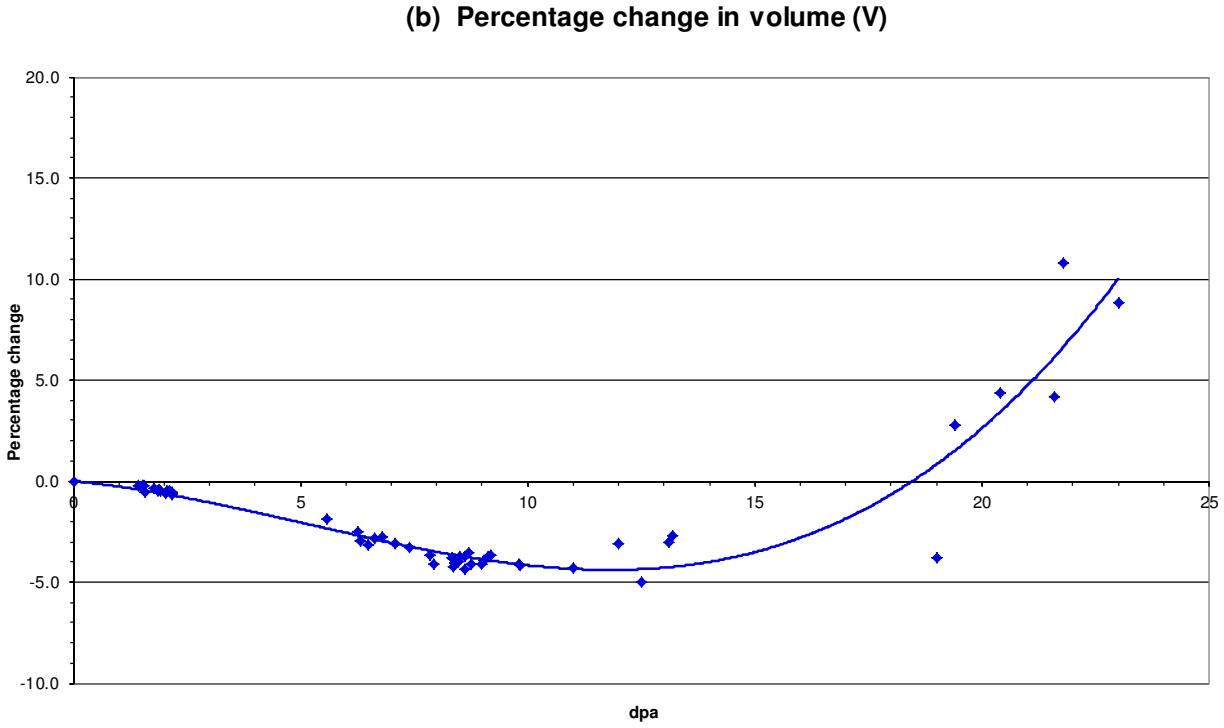

Figure 8 - Dimensional change and volume change for PCEA

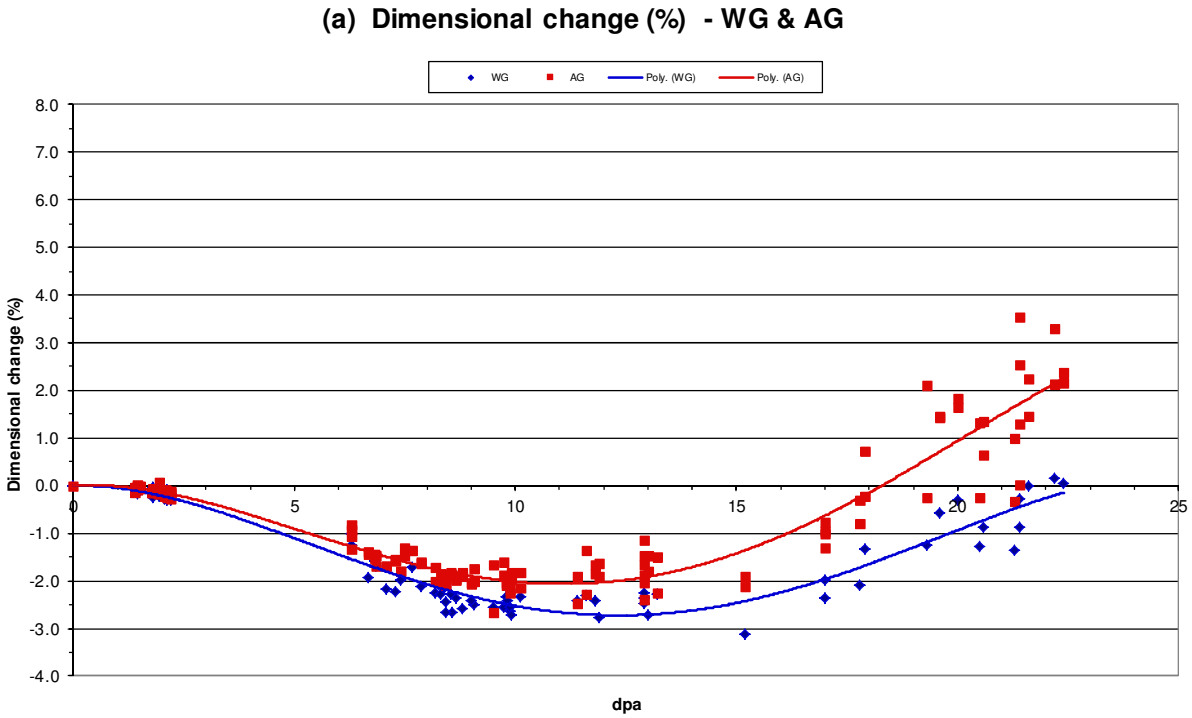

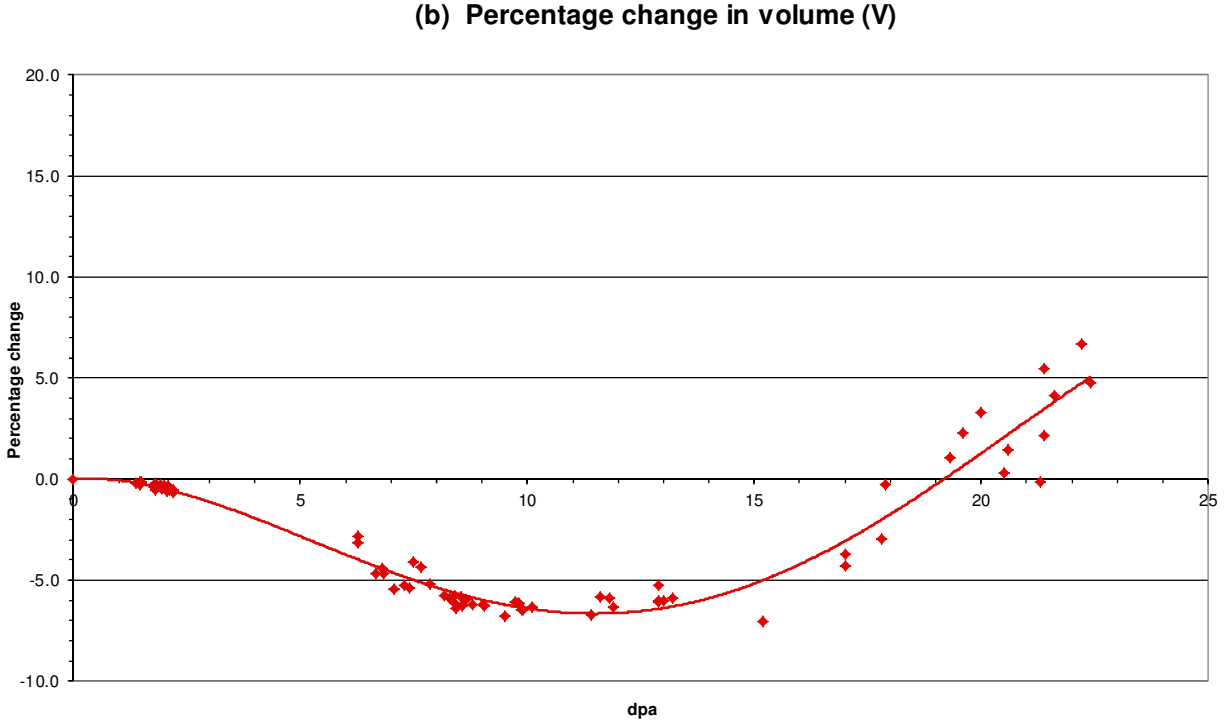

Figure 9 - Dimensional change and volume change for PPEA

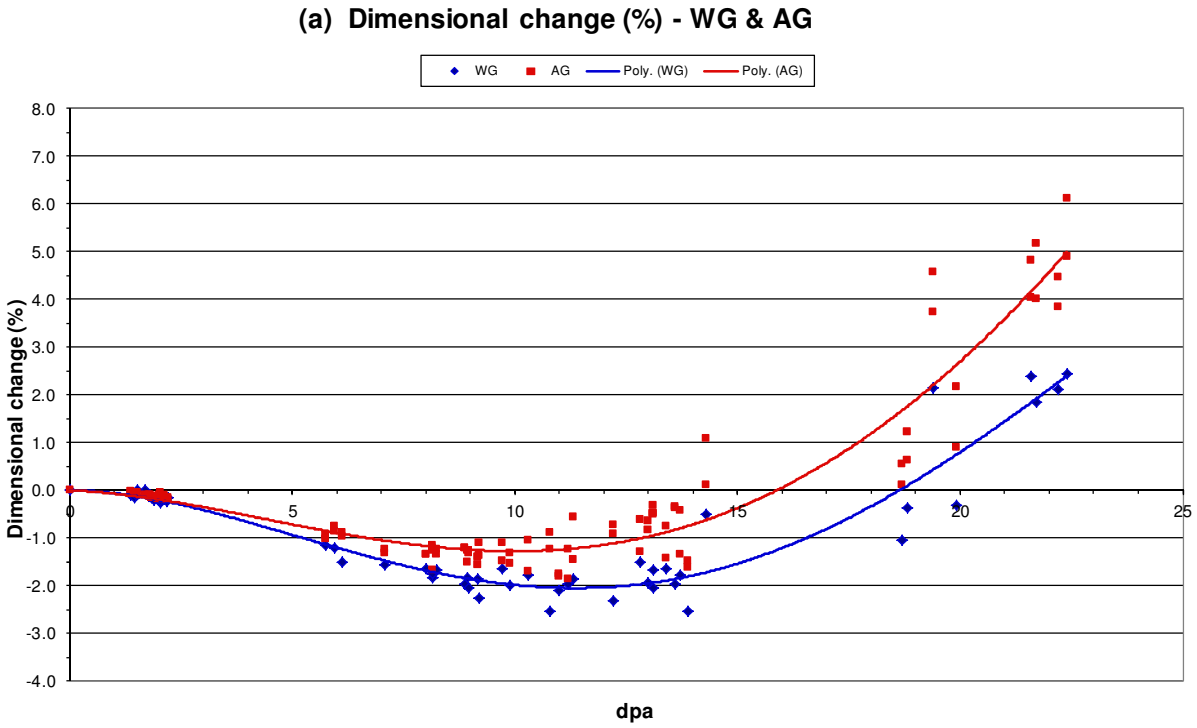

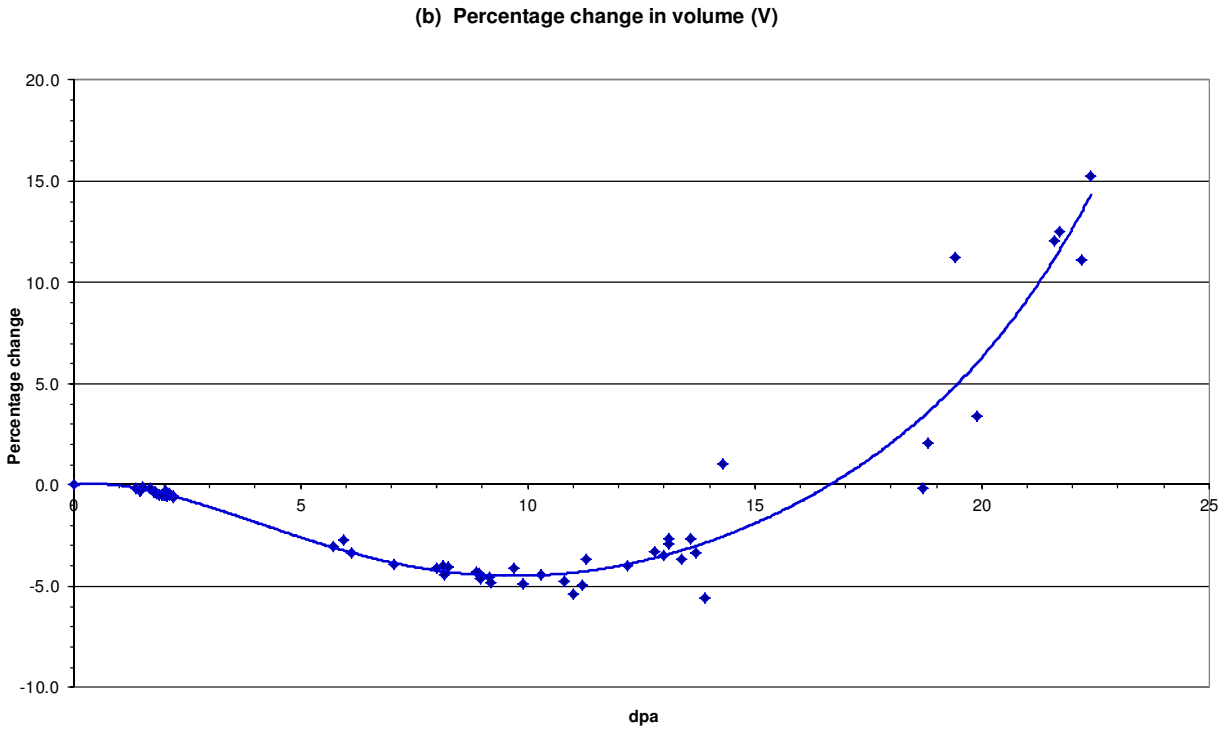

Figure 10 - Dimensional change and volume change for PCIB

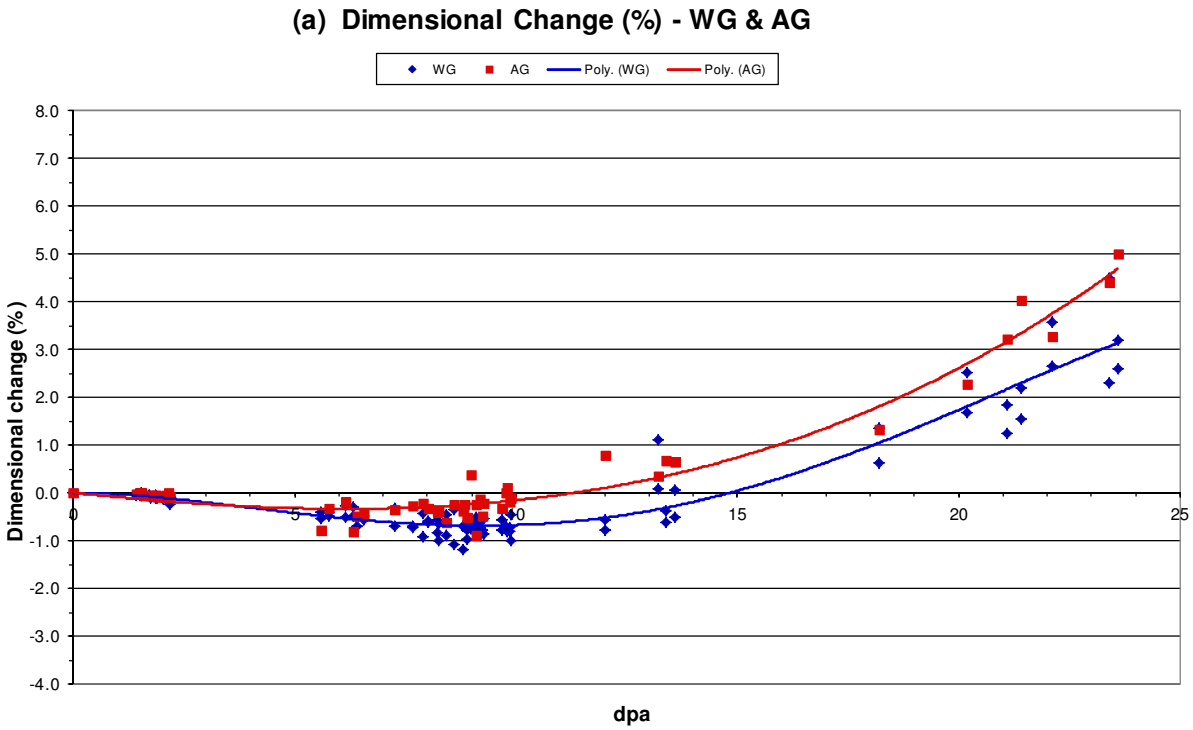

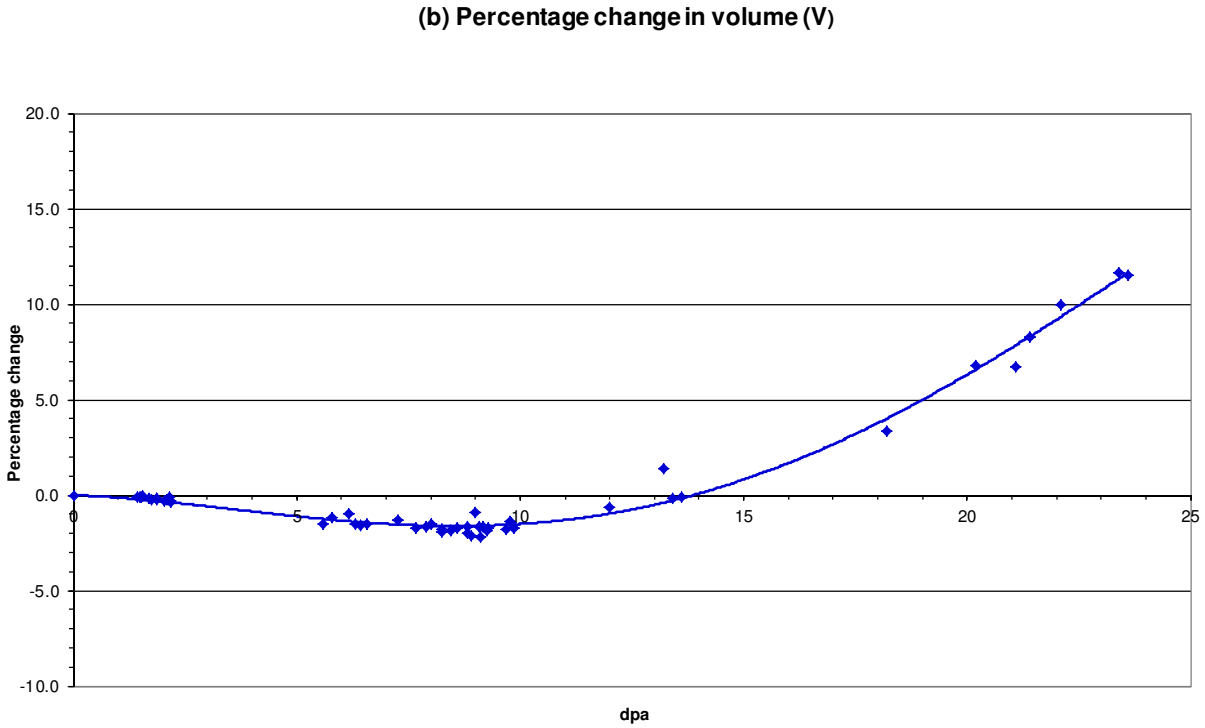

Figure 11 - Dimensional change and volume change for IG-110

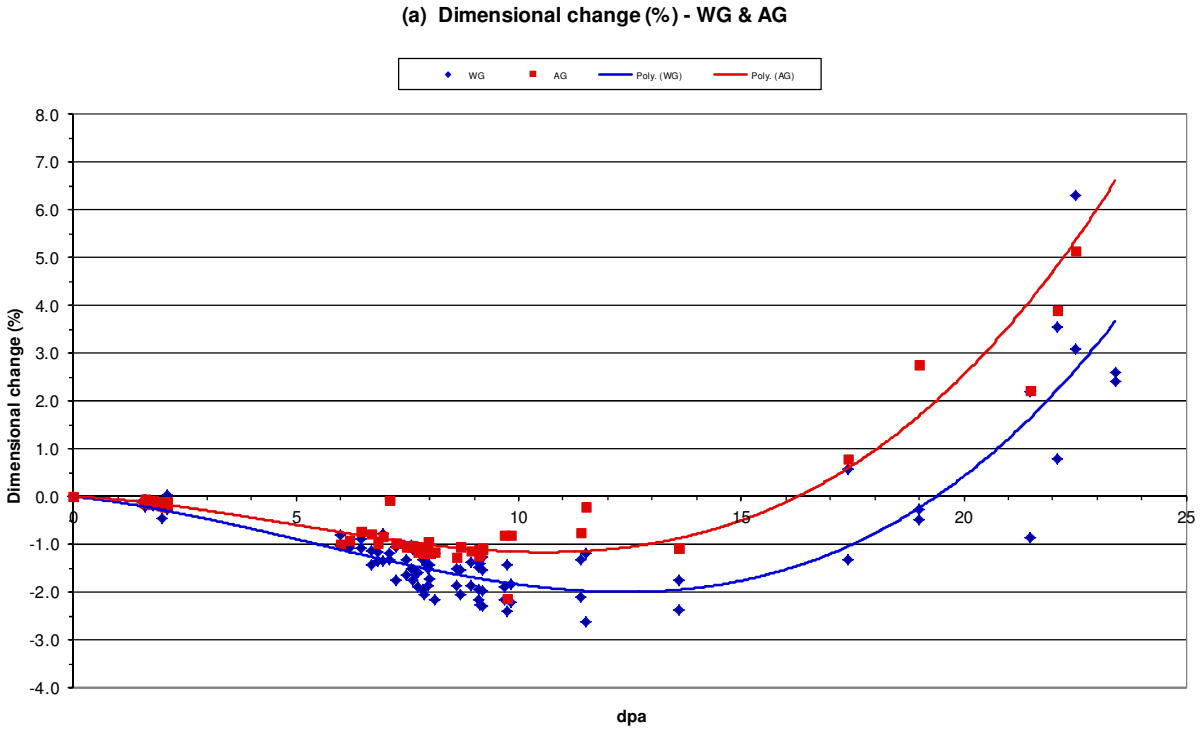

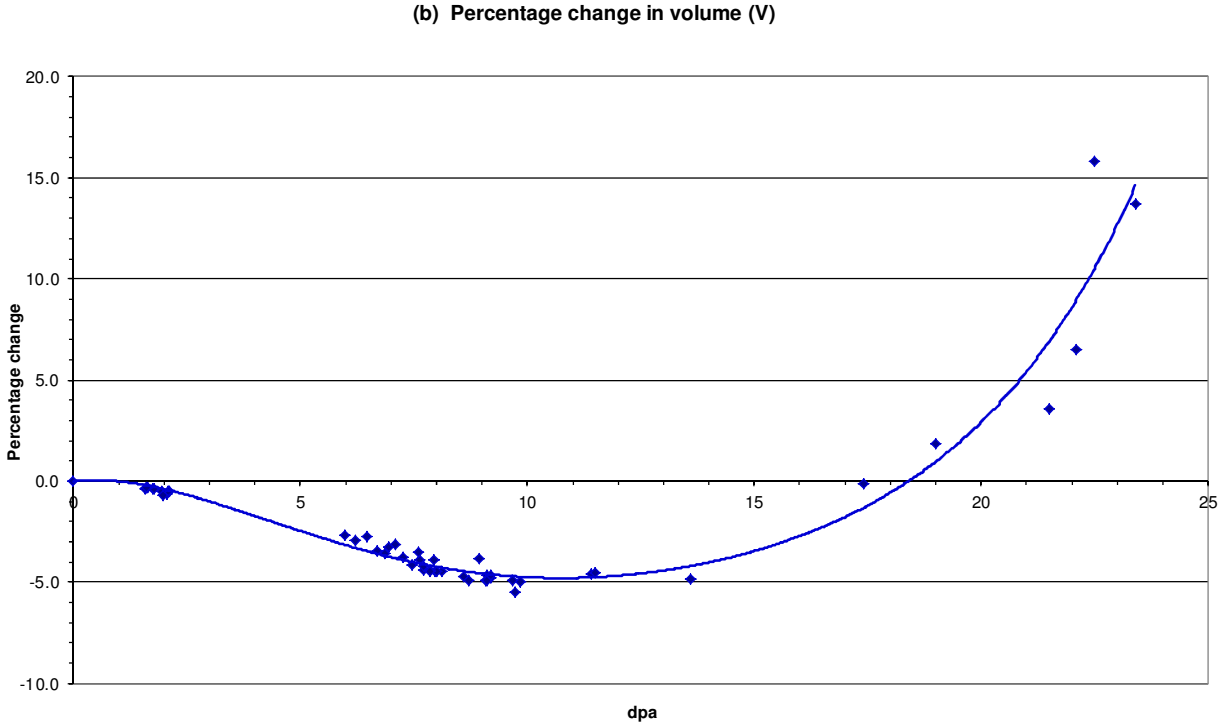

Figure 12 - Dimensional change and volume change for IG-430

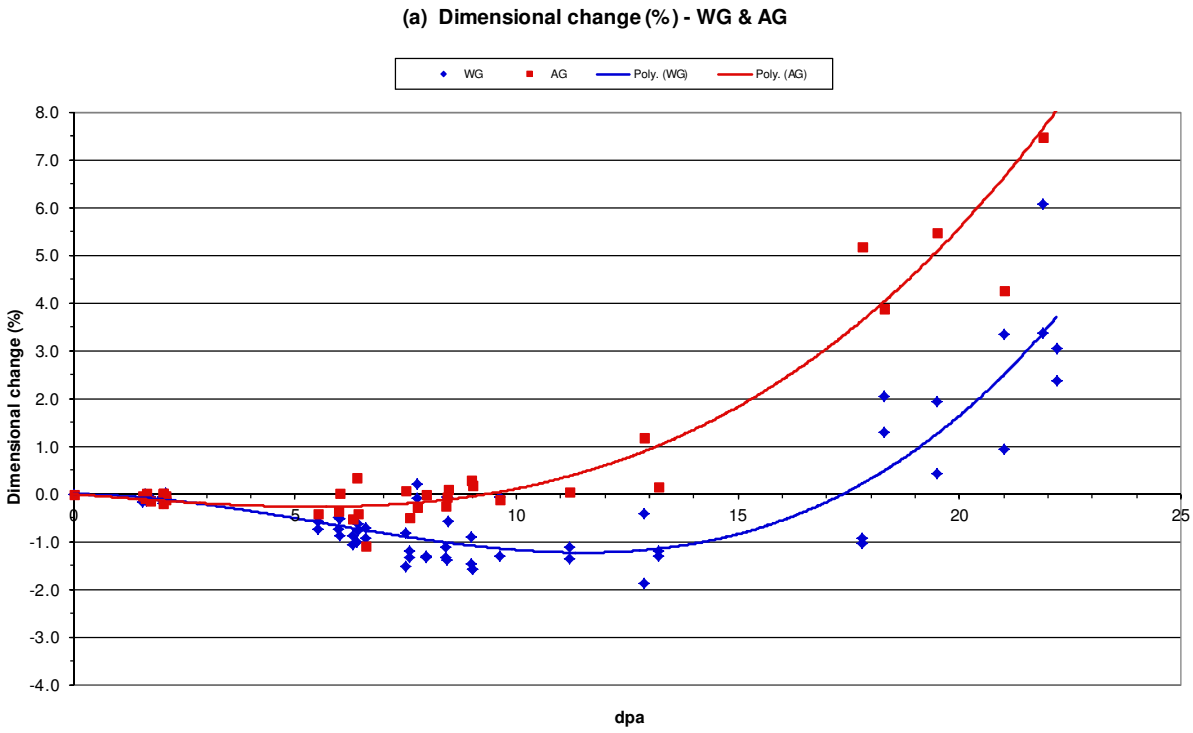

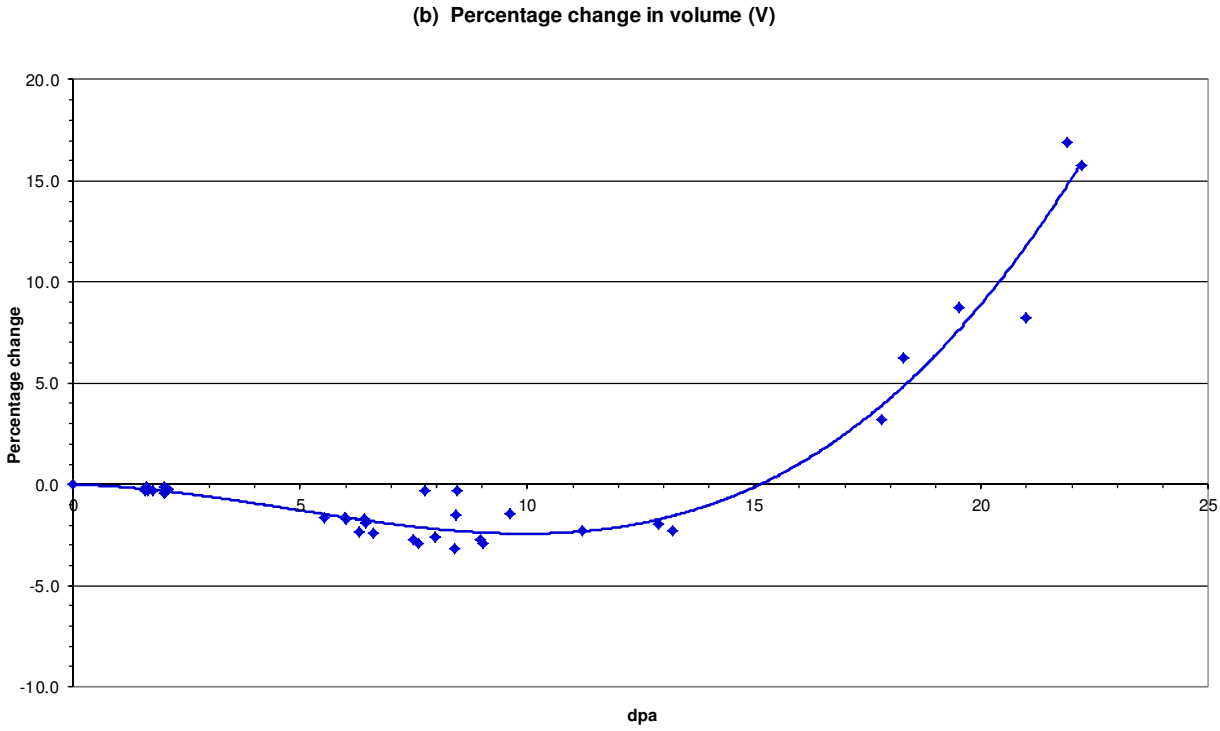

Figure 13 - DYM change for NBG-10

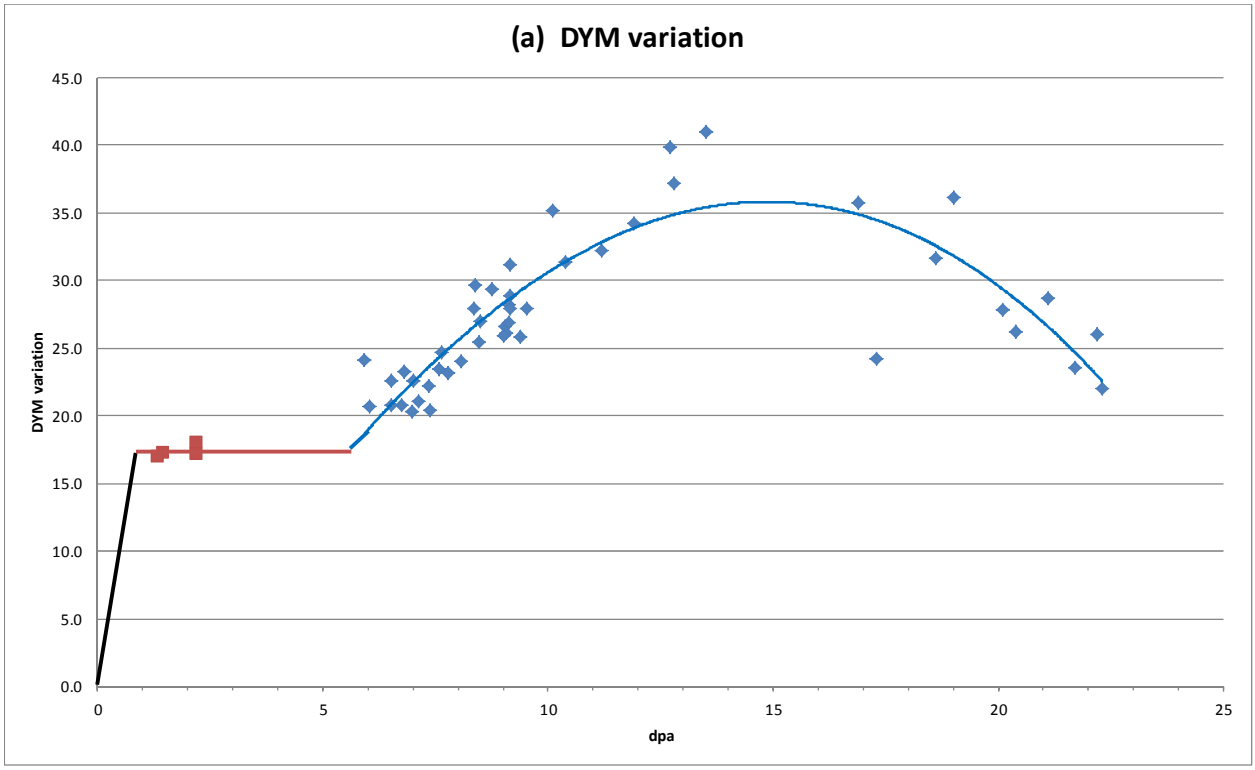

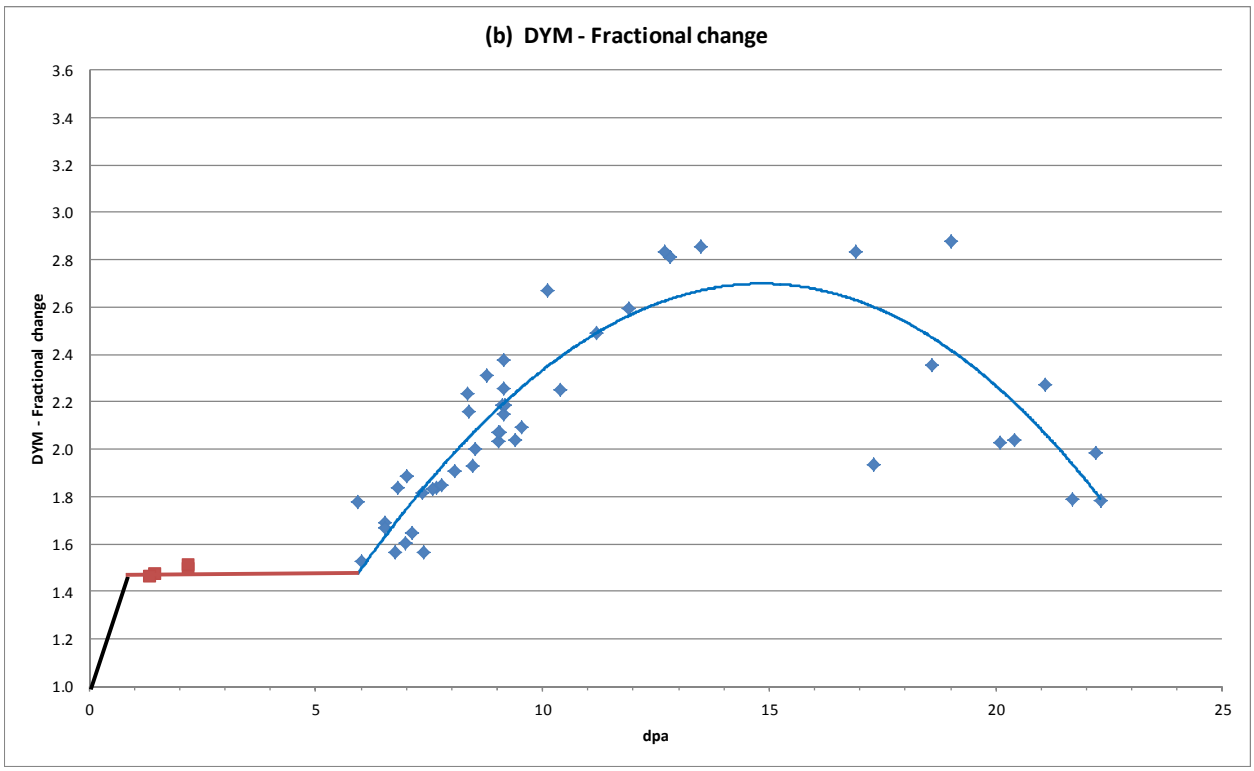

Figure 14 - DYM change for NBG-25

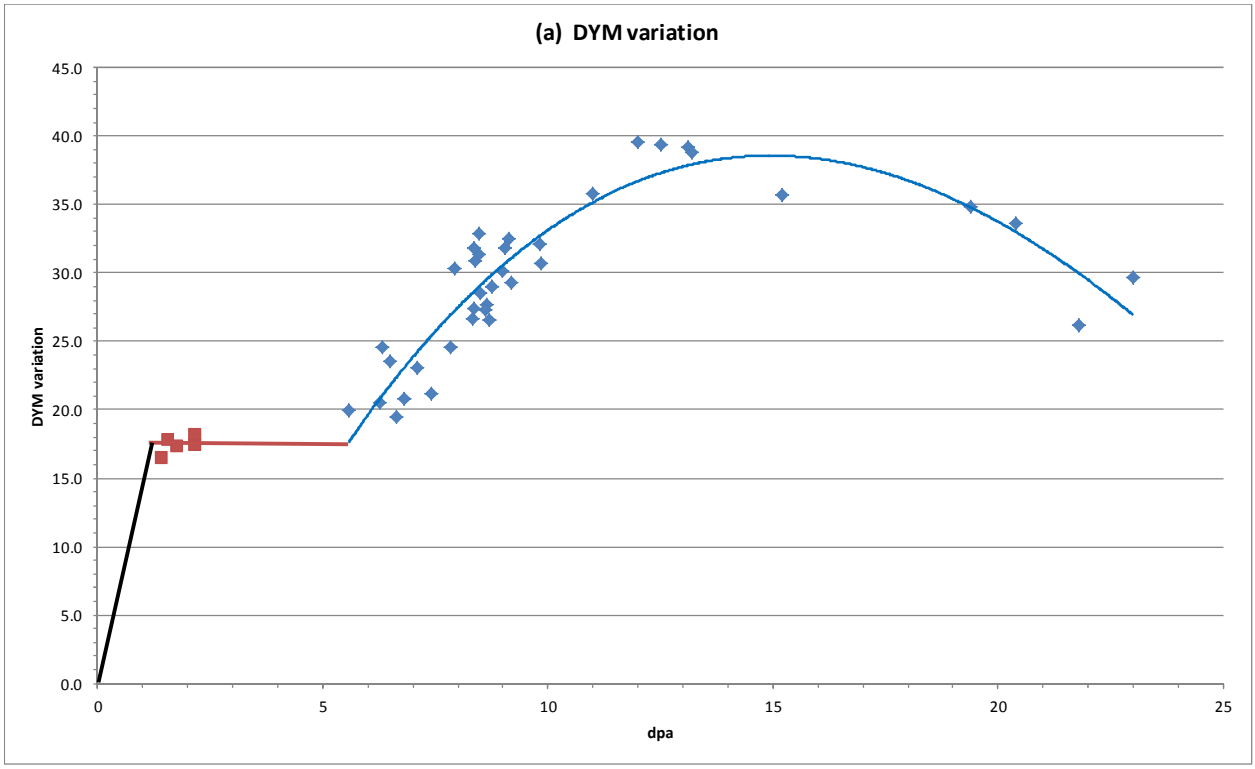

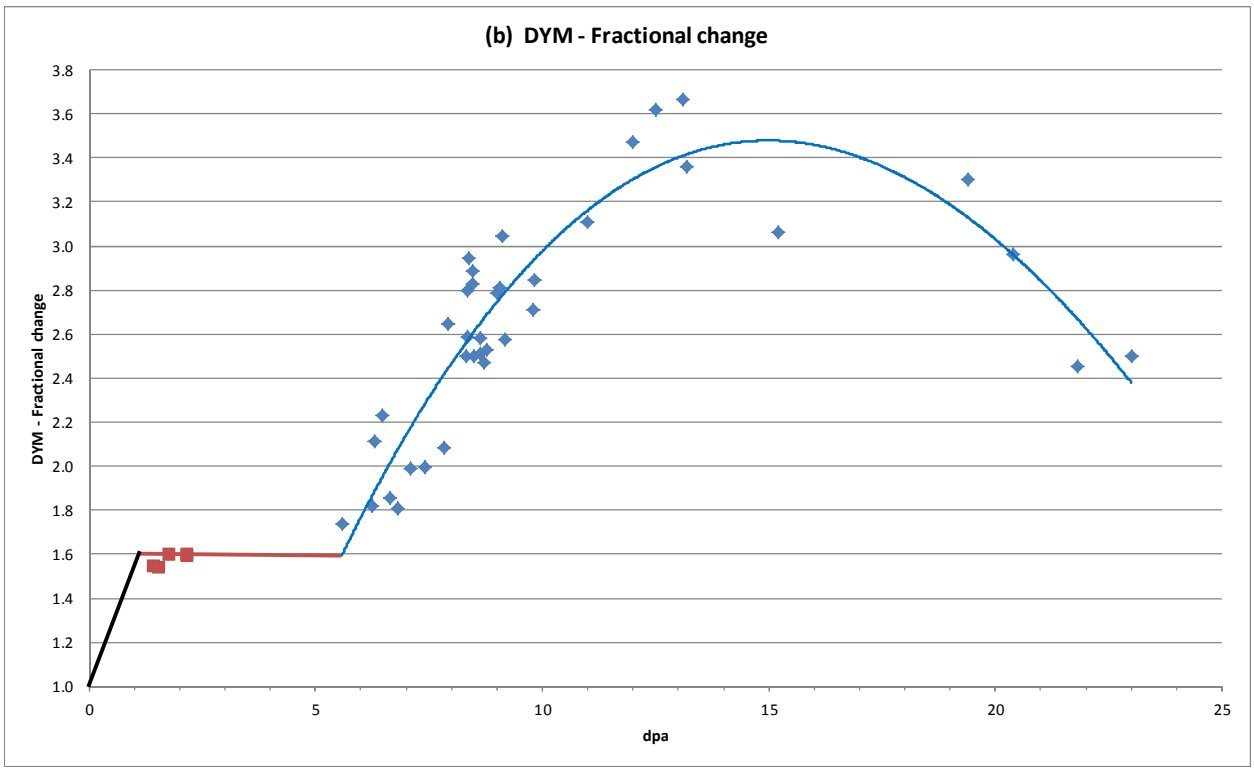

Figure 15- DYM change for PCEA

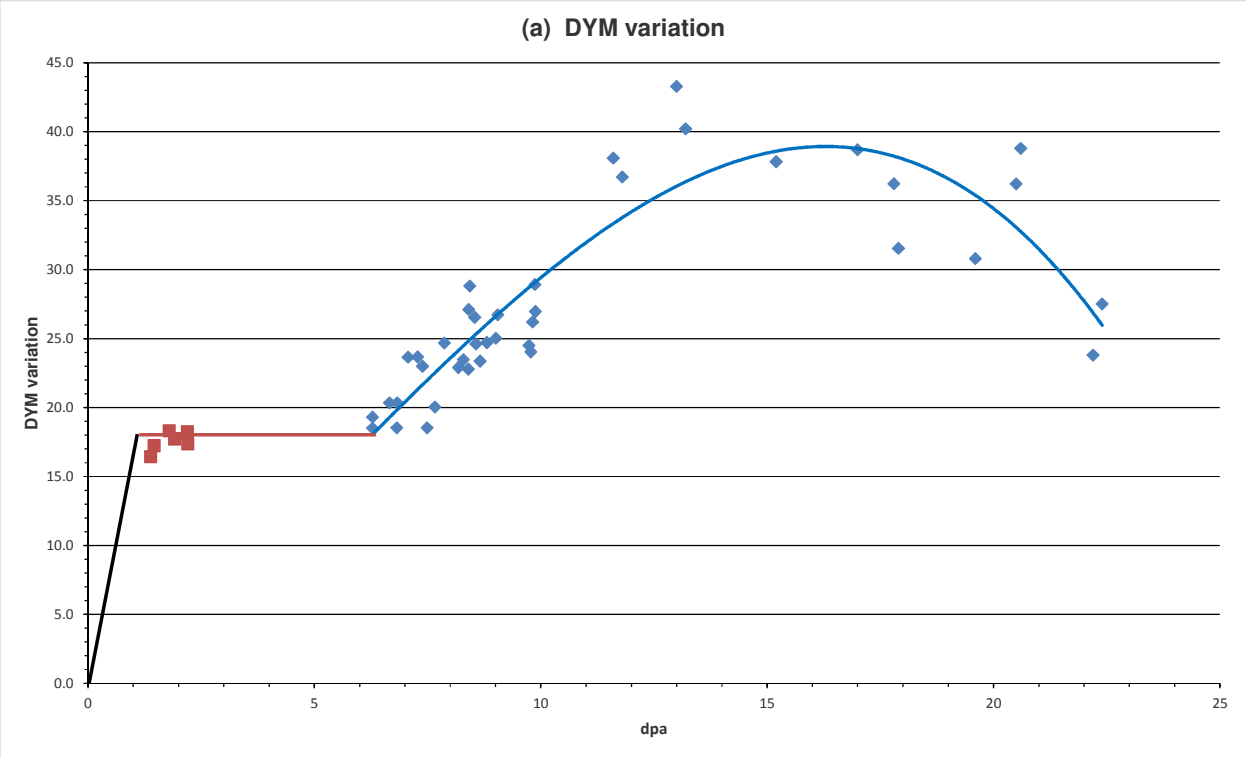

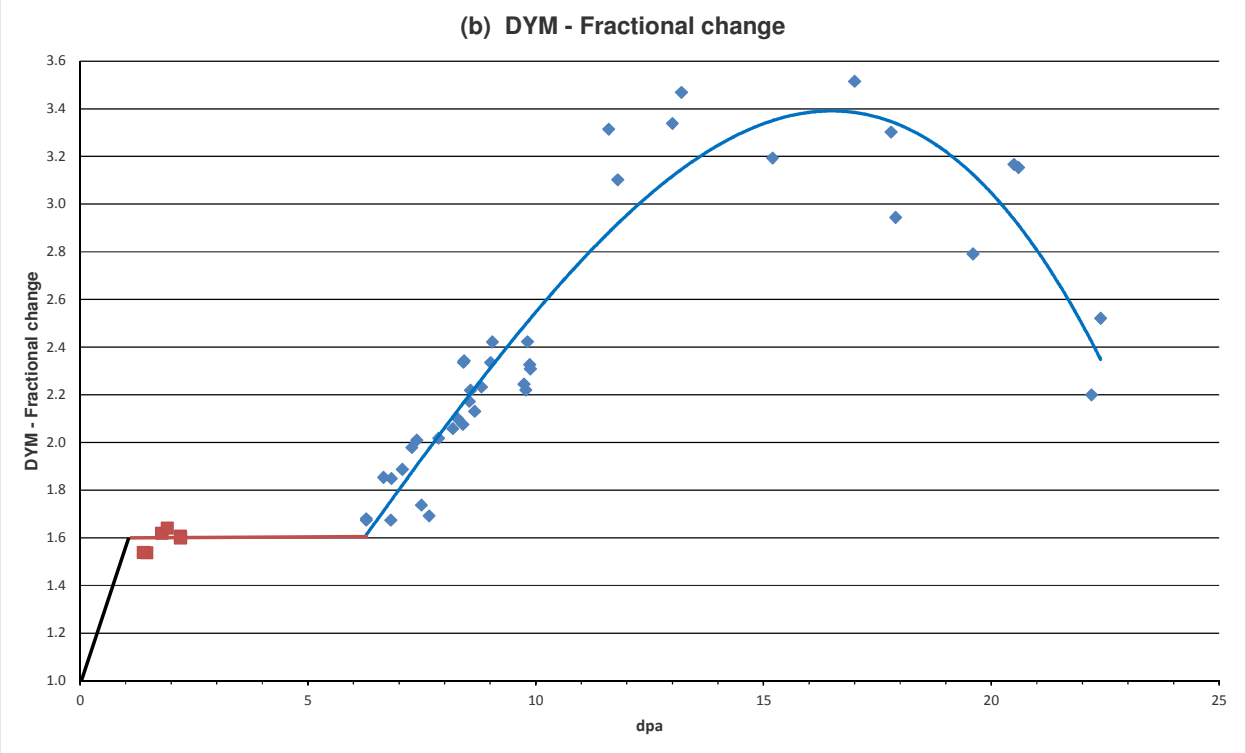

Figure 16- DYM change for PPEA

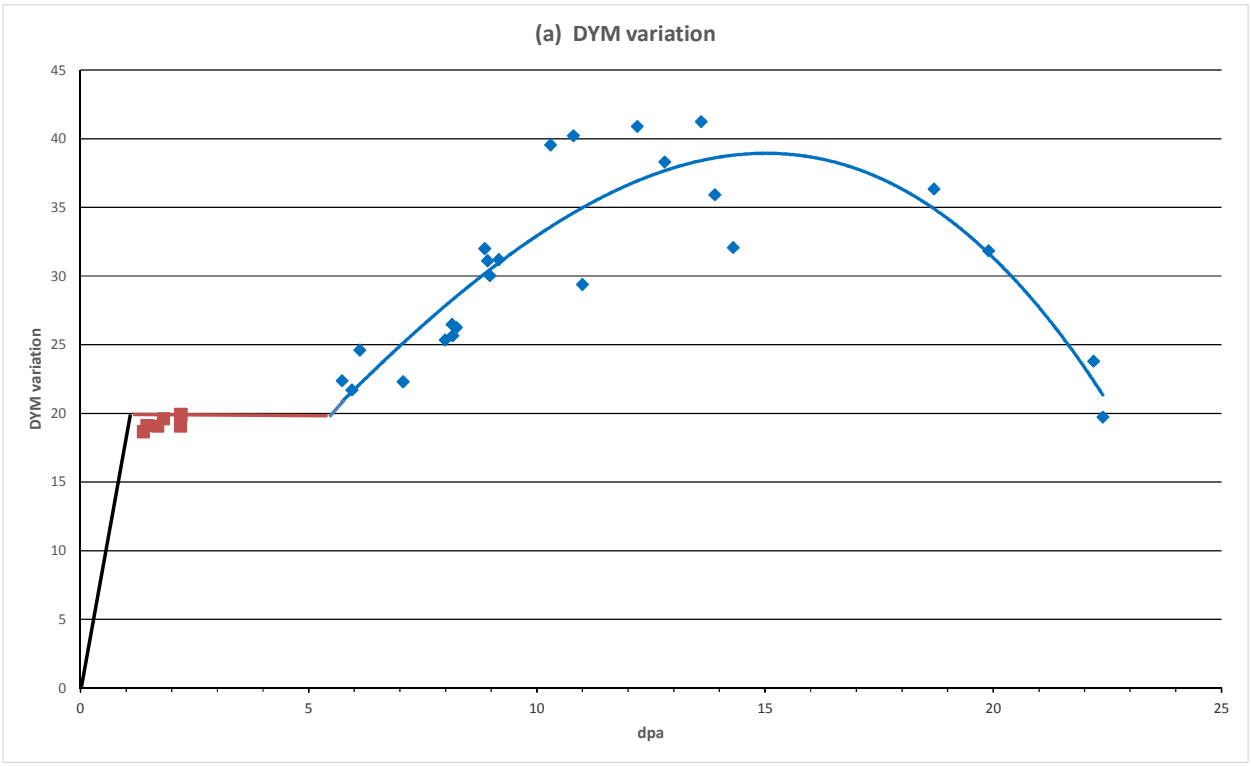

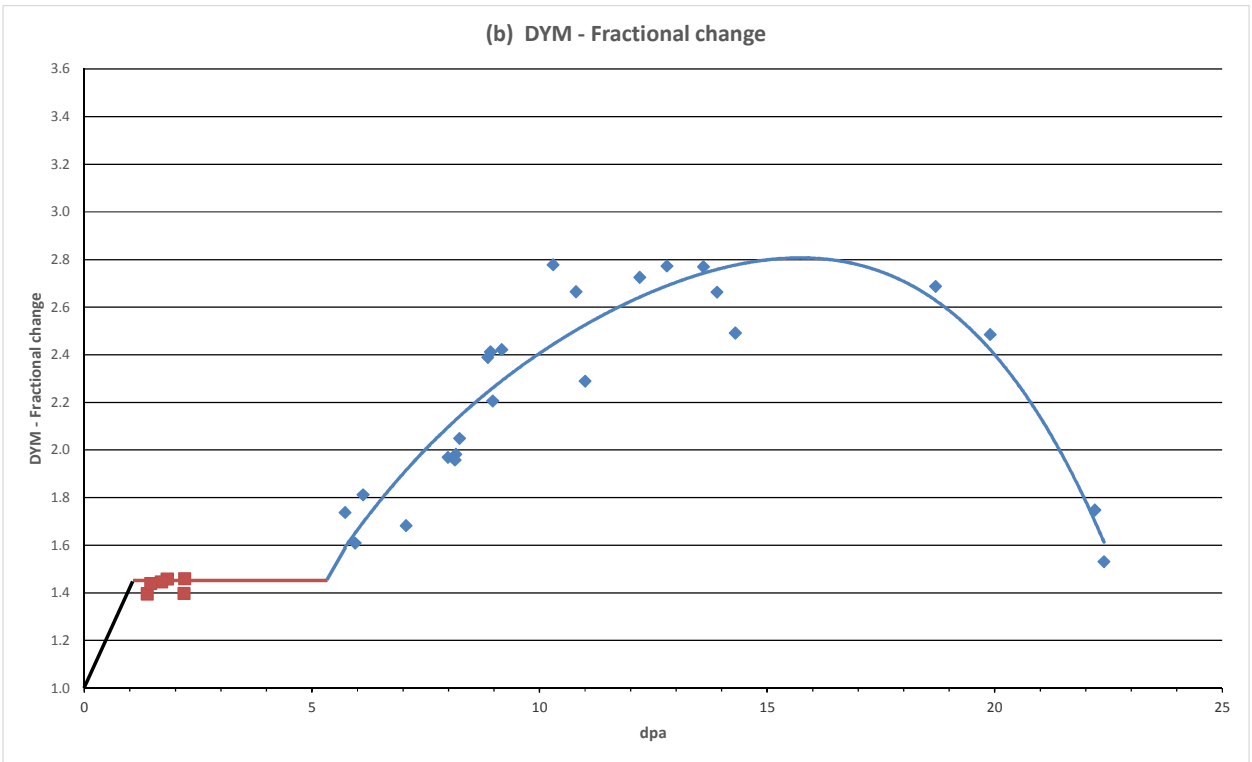

Figure 17- DYM change for PCIB

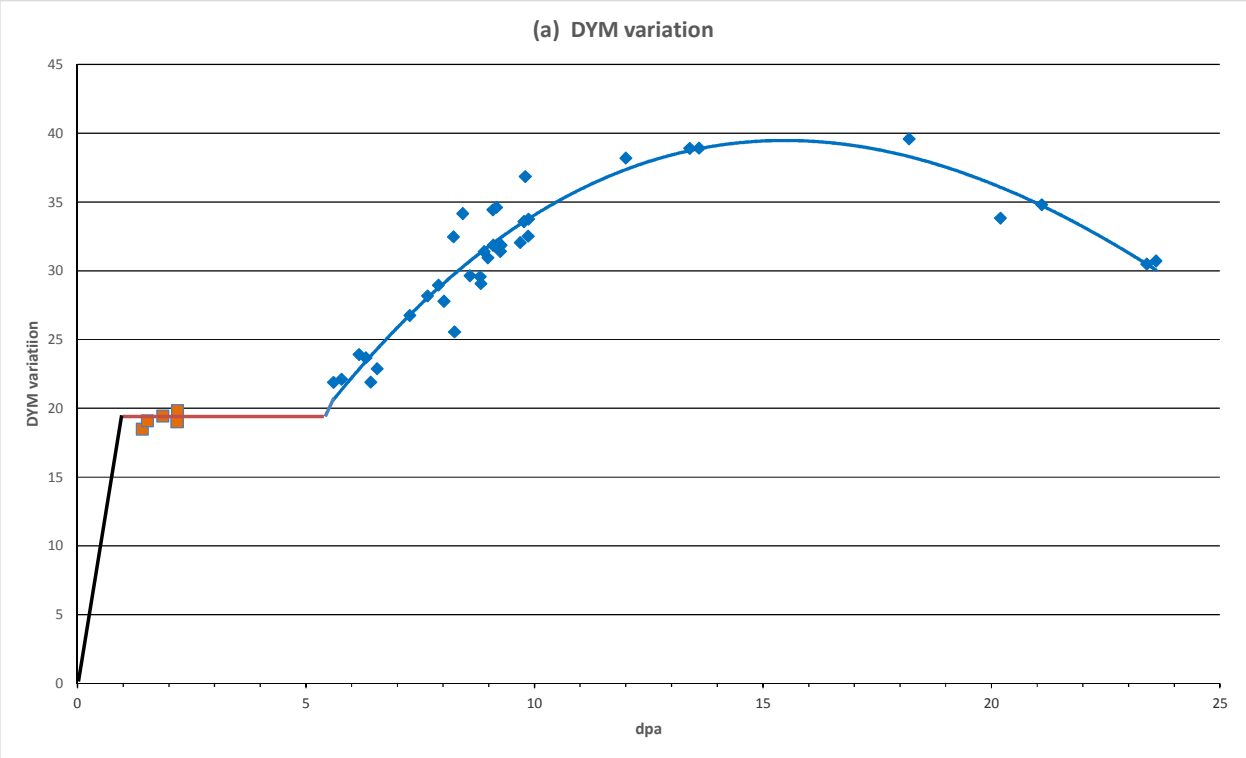

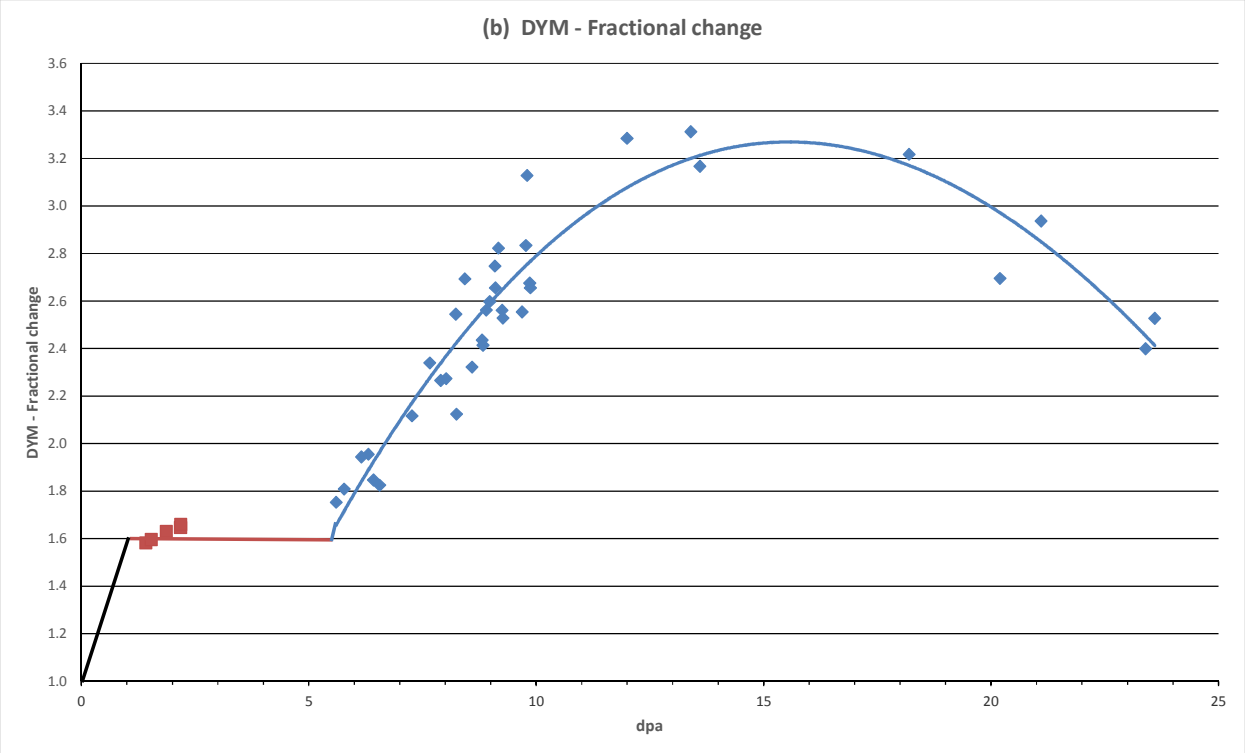

Figure 18- DYM change for IG-110

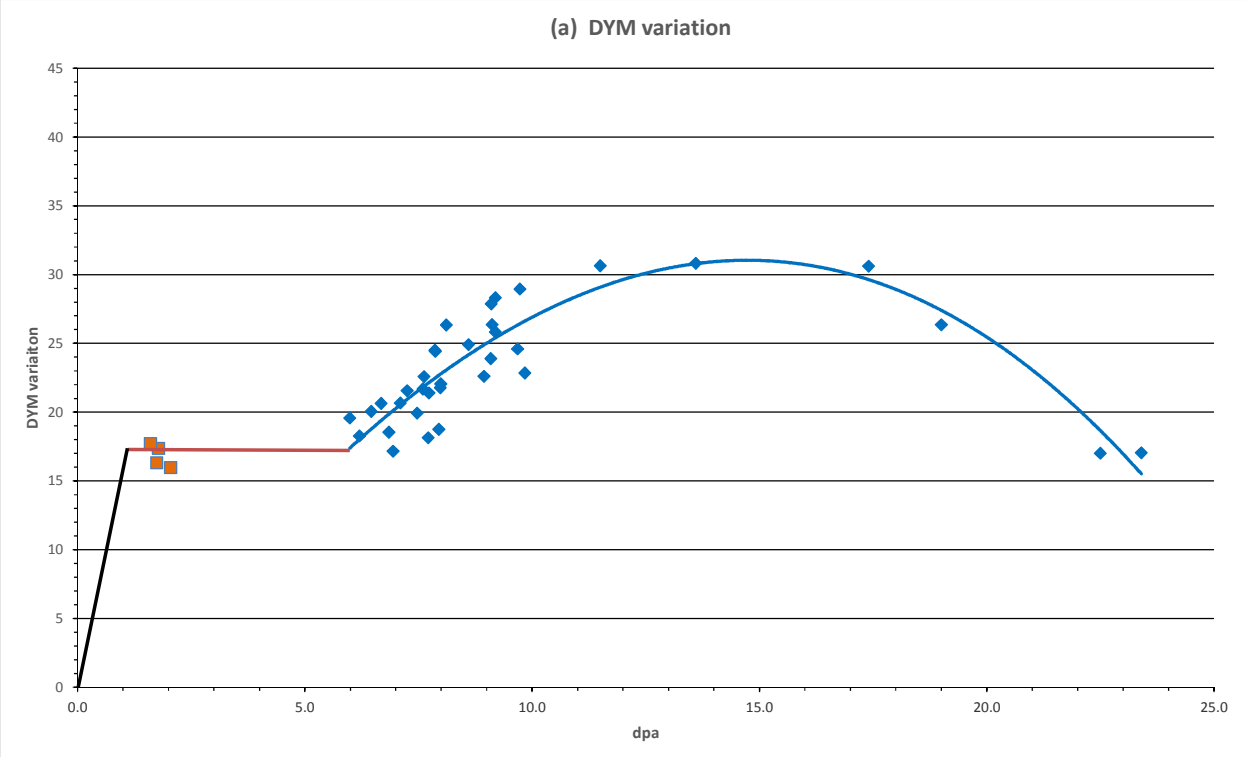

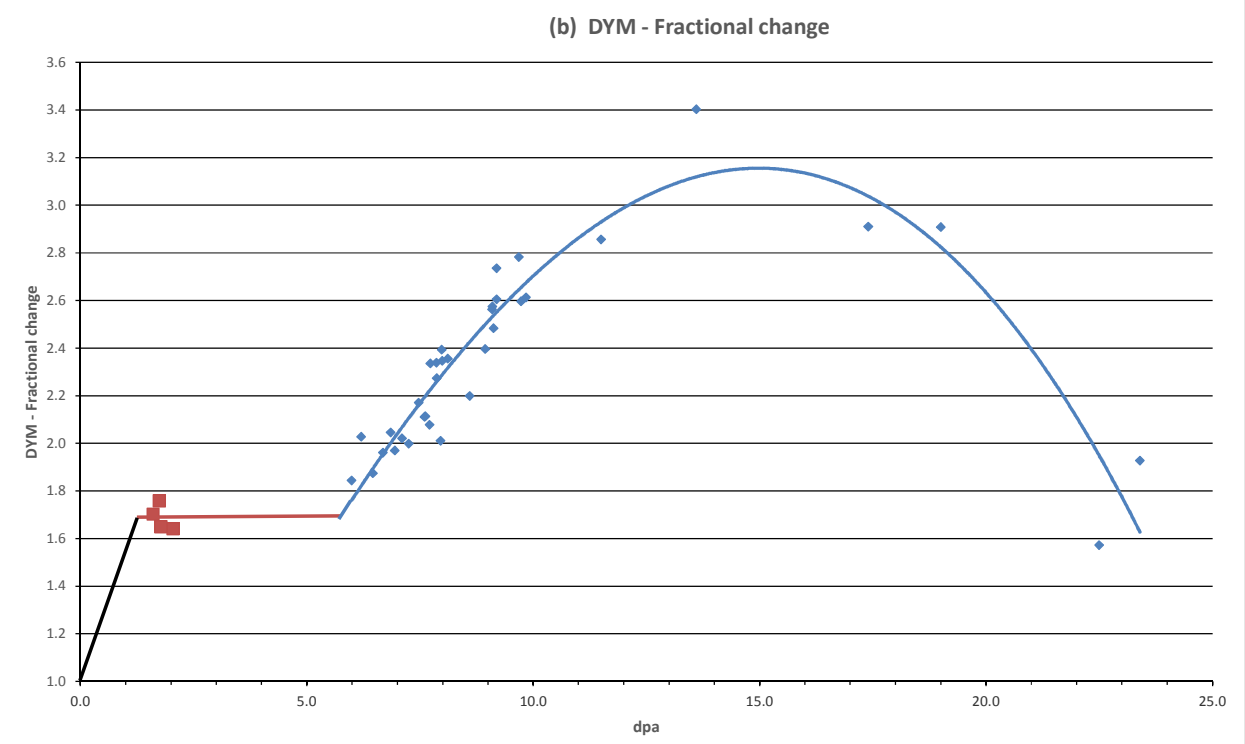

Figure 19- DYM change for IG-430

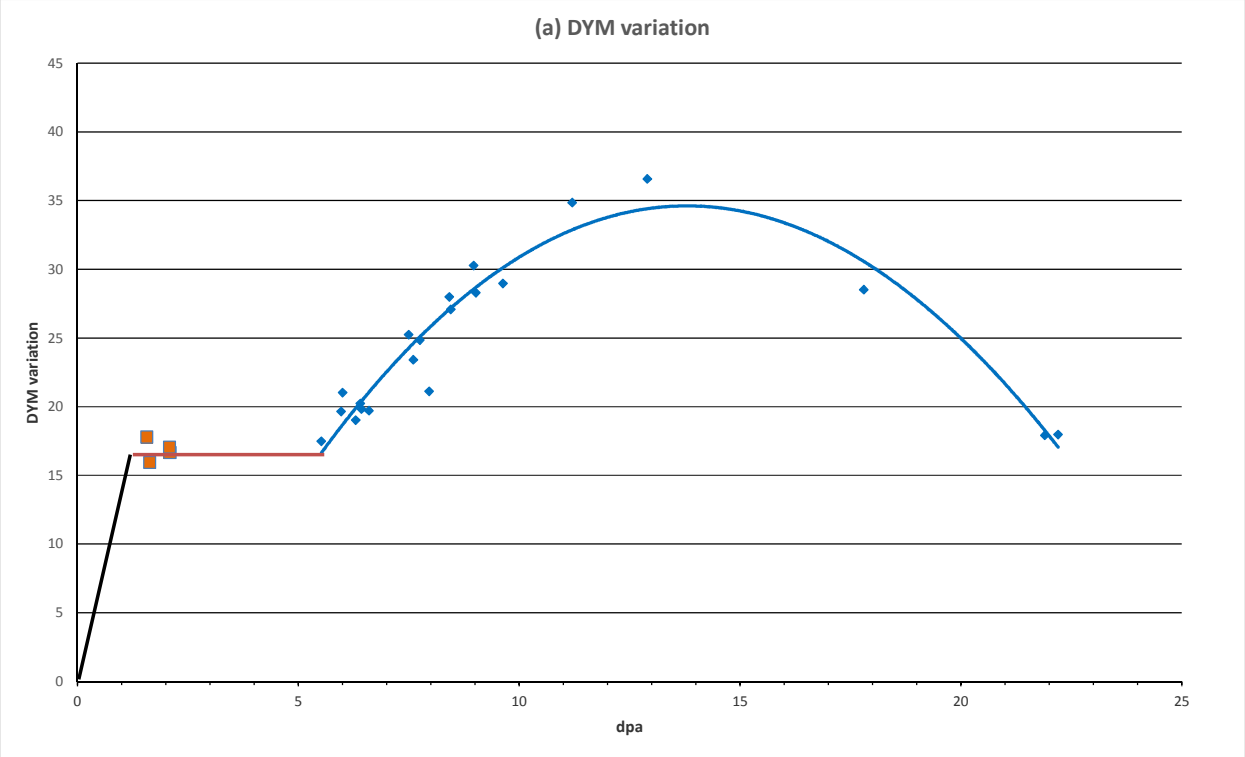

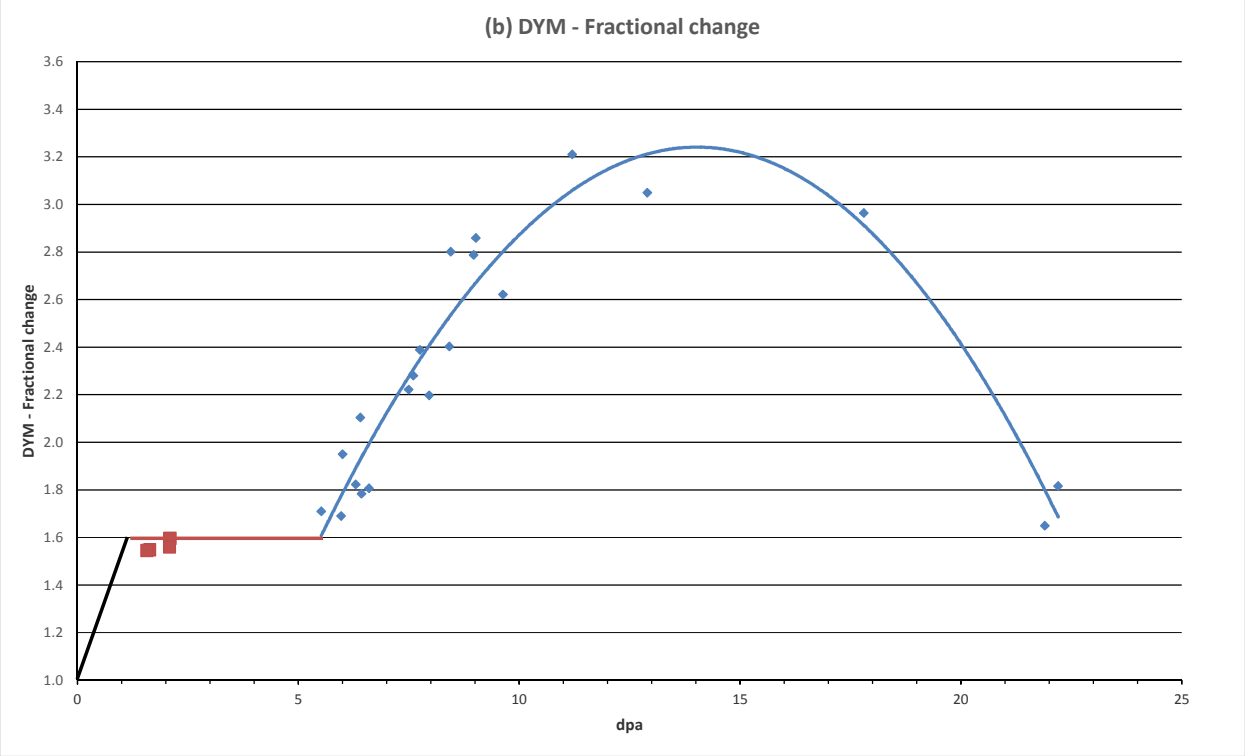

Figure 20 - CTE change for NBG-10

(a) CTE variation

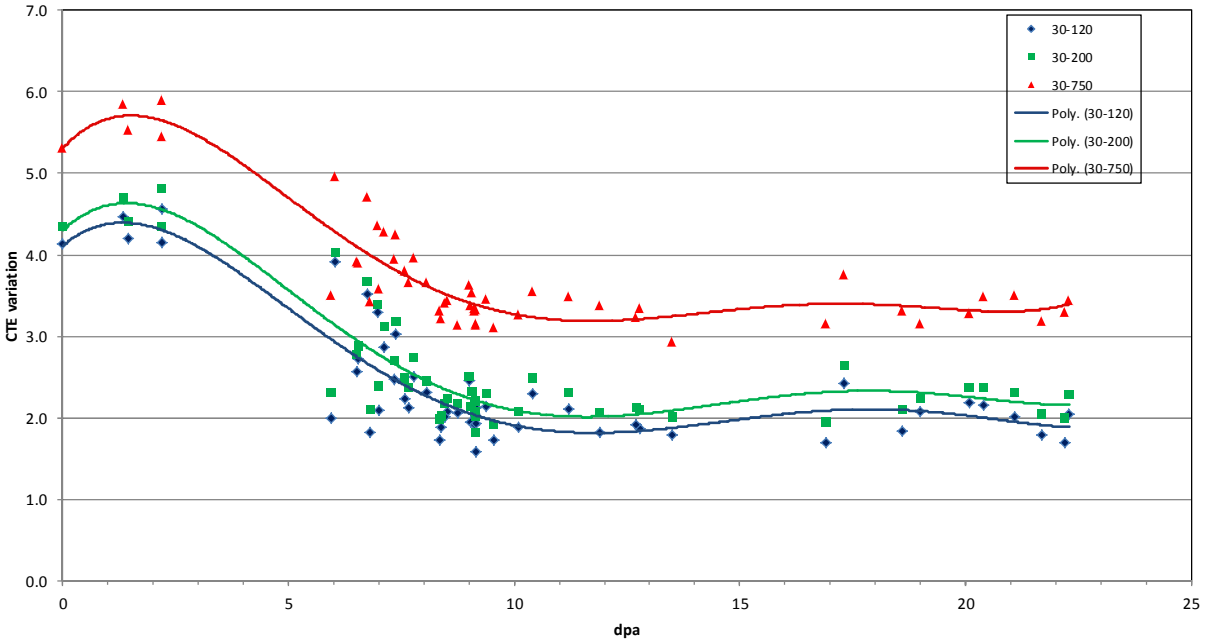

(b) CTE - Fractional change

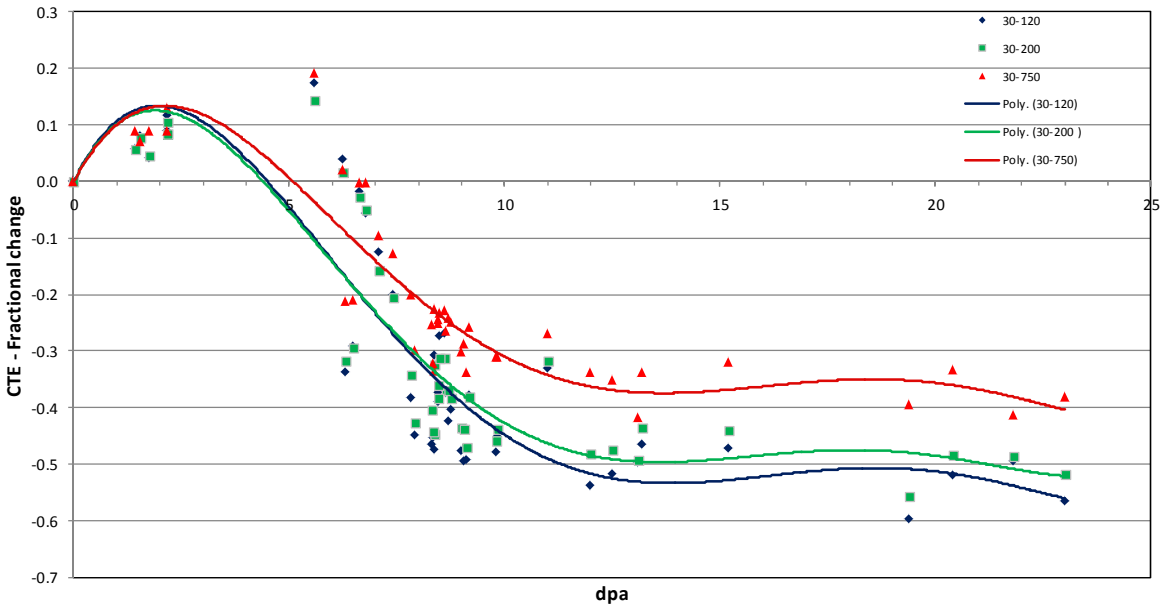

Figure 21 - CTE change for NBG-25

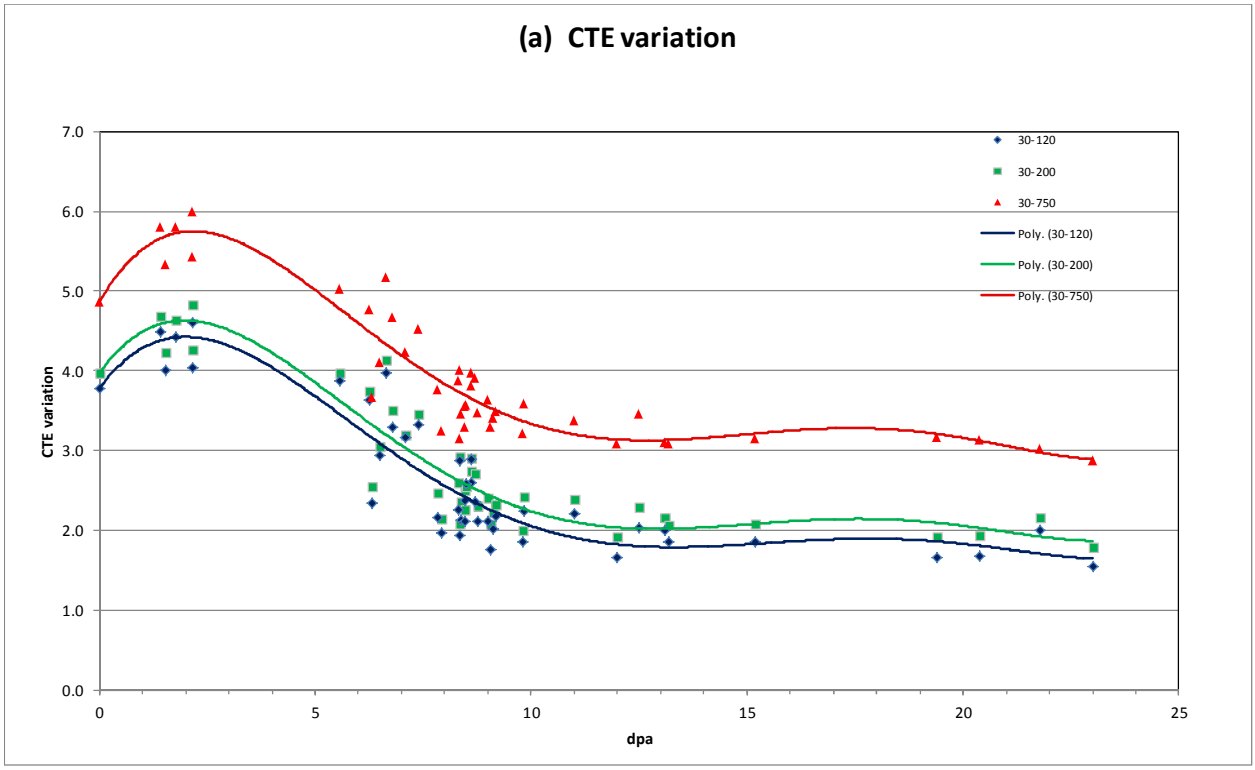

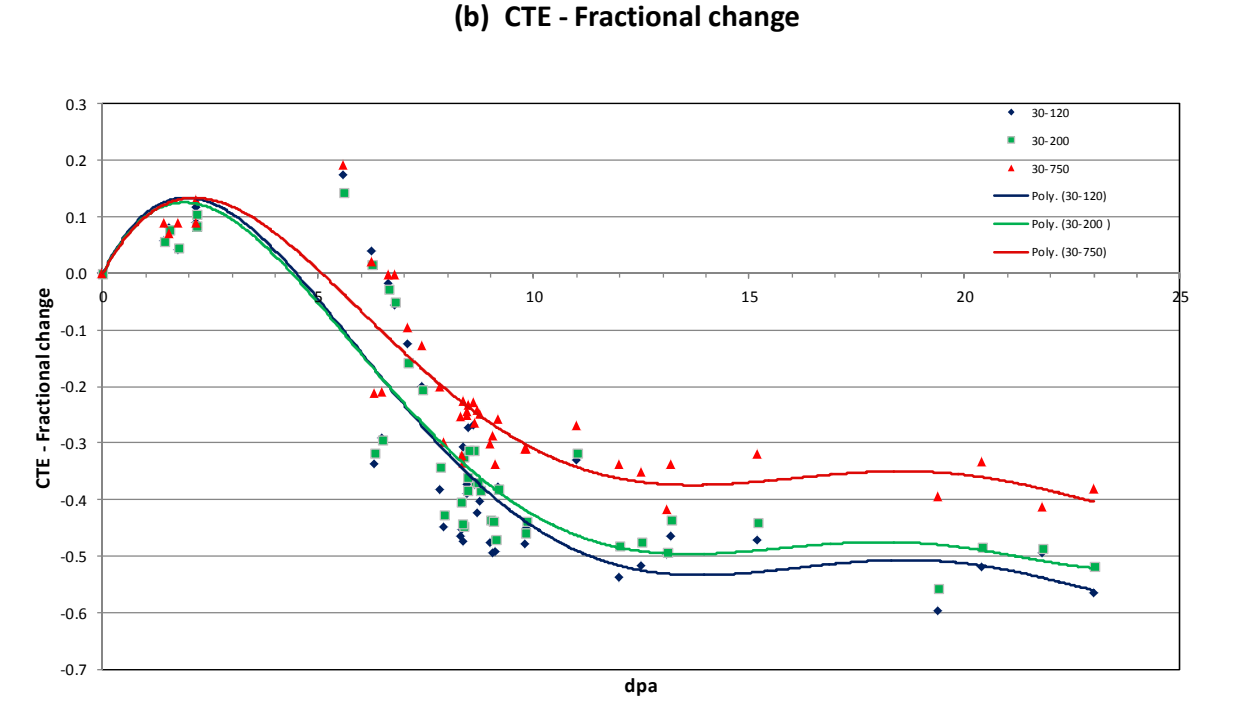

Figure 22- CTE change for PCEA

(a) CTE variation

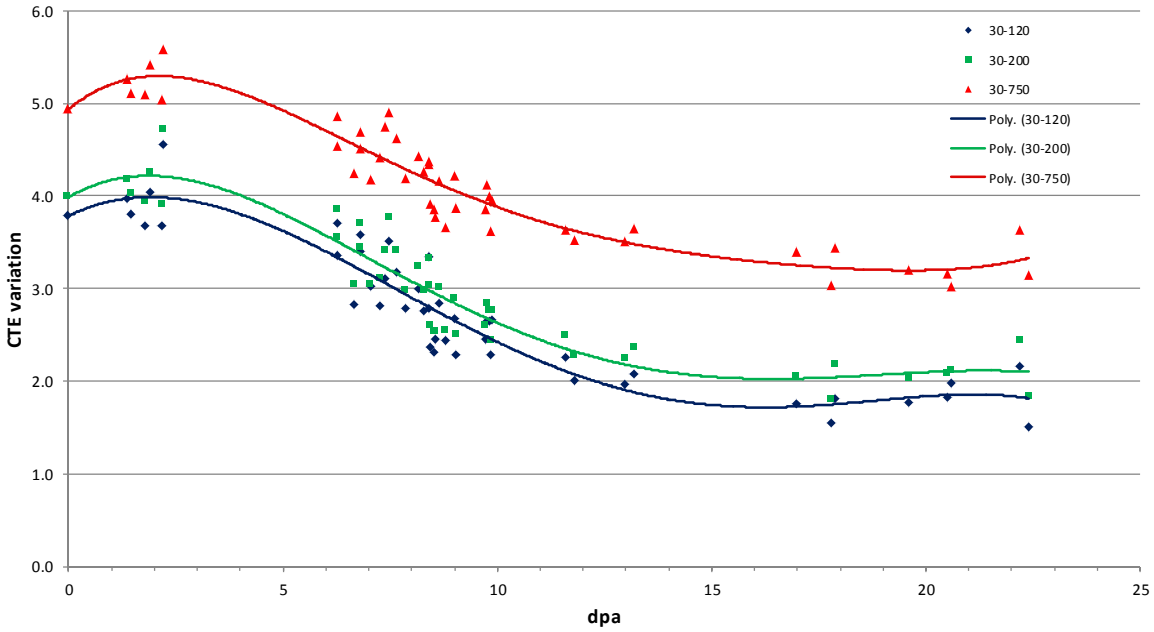

(b) CTE - Fractional change

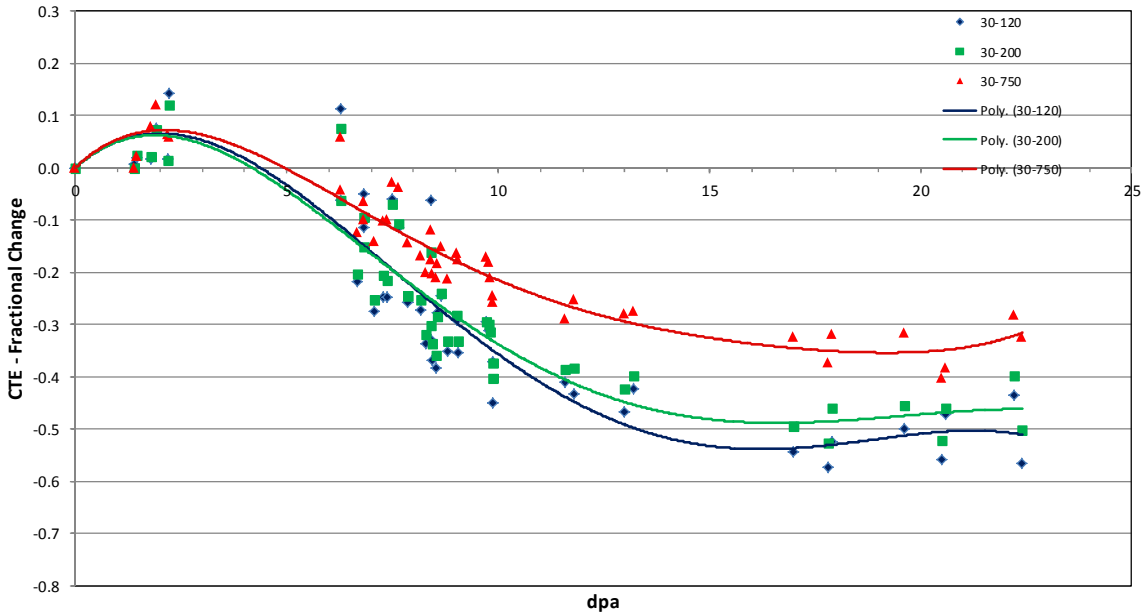

Figure 23- CTE change for PPEA

(a) CTE variation

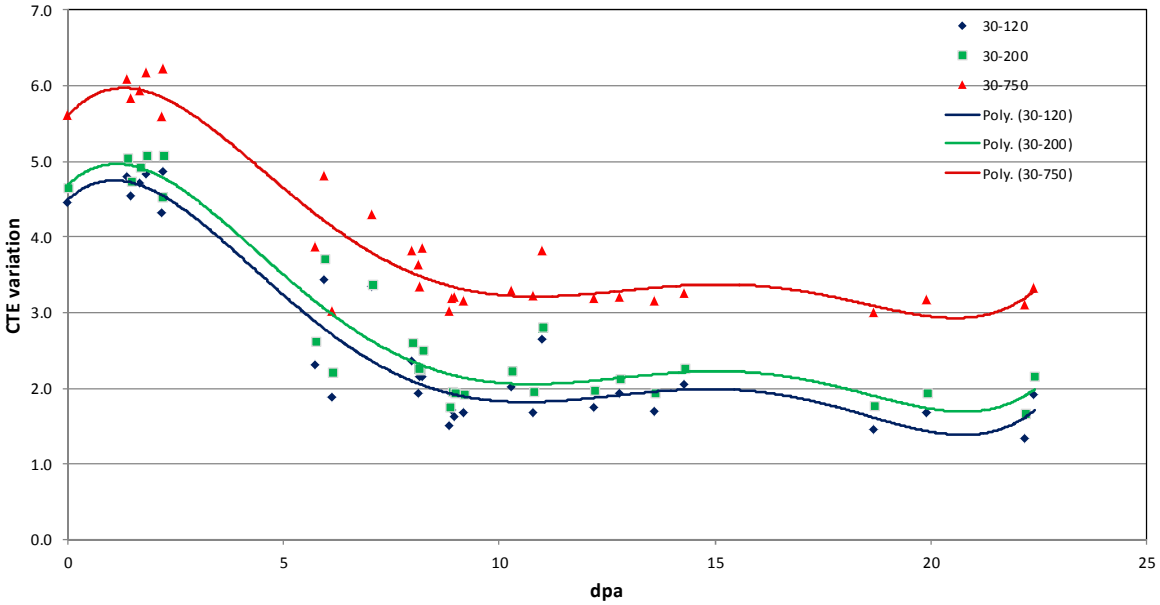

(b) CTE - Fractional change

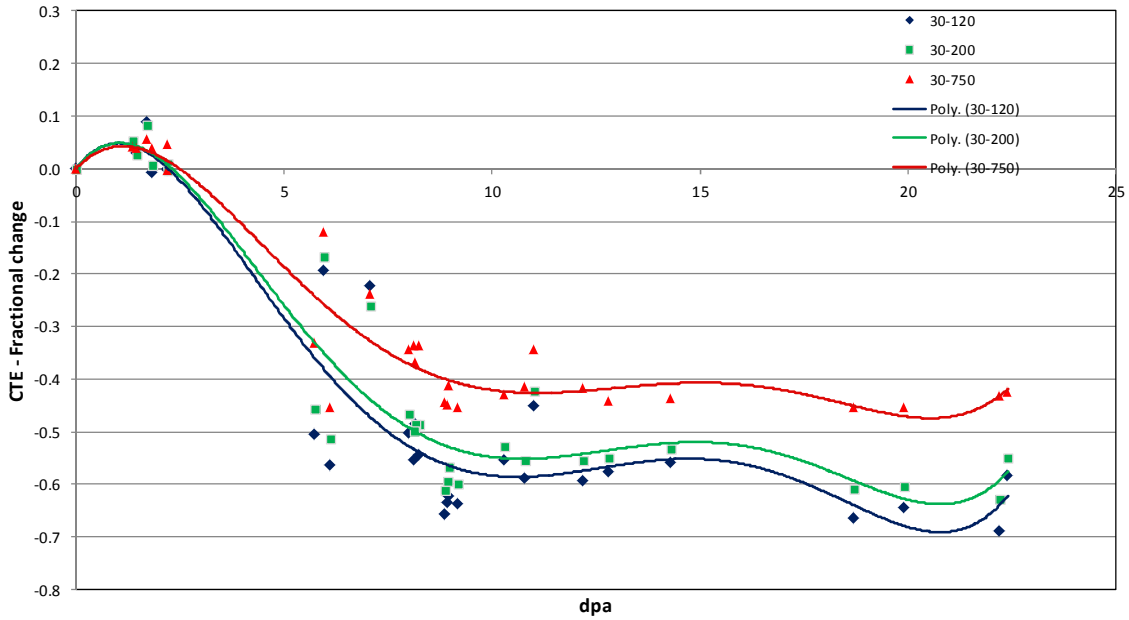

Figure 24- CTE change for PCIB

(a) CTE variation

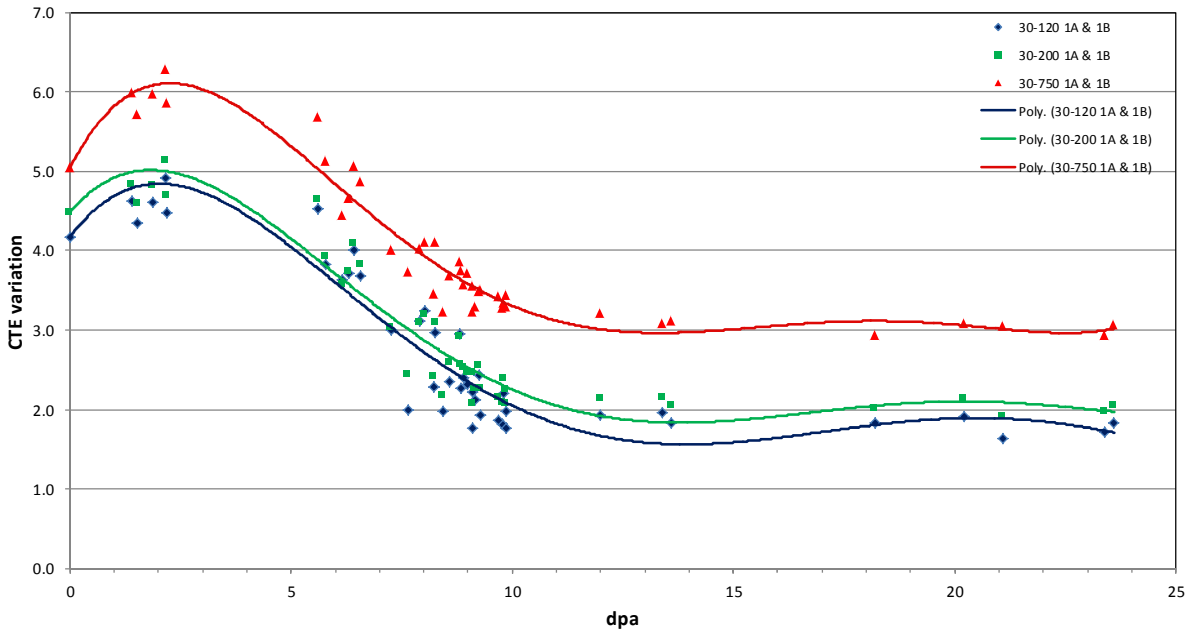

(b) CTE -Fractional change

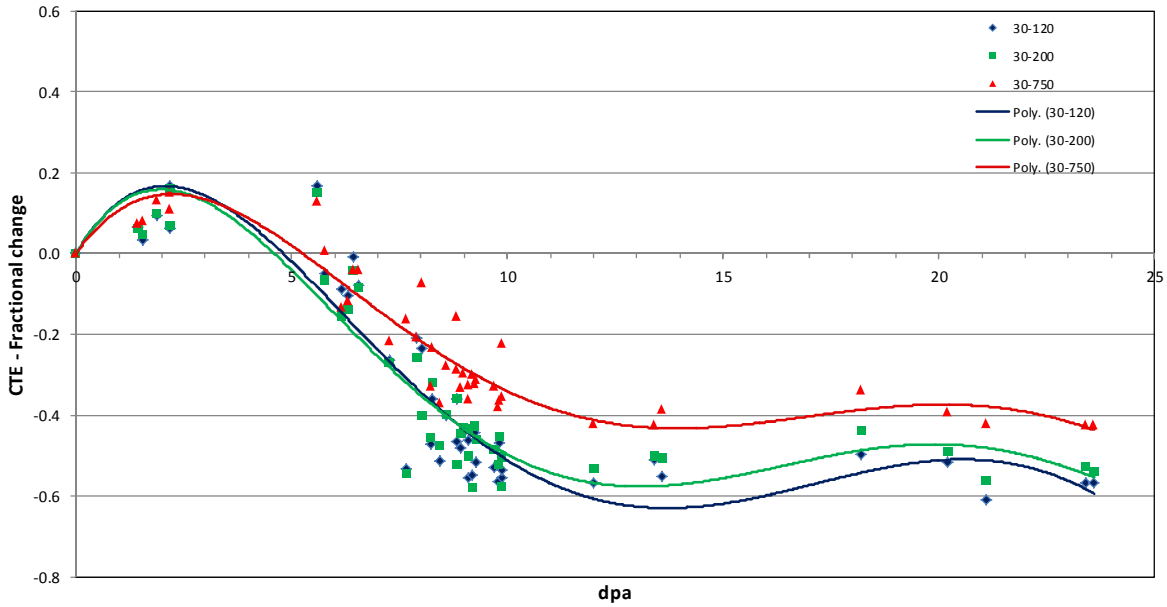

Figure 25- CTE change for IG-110

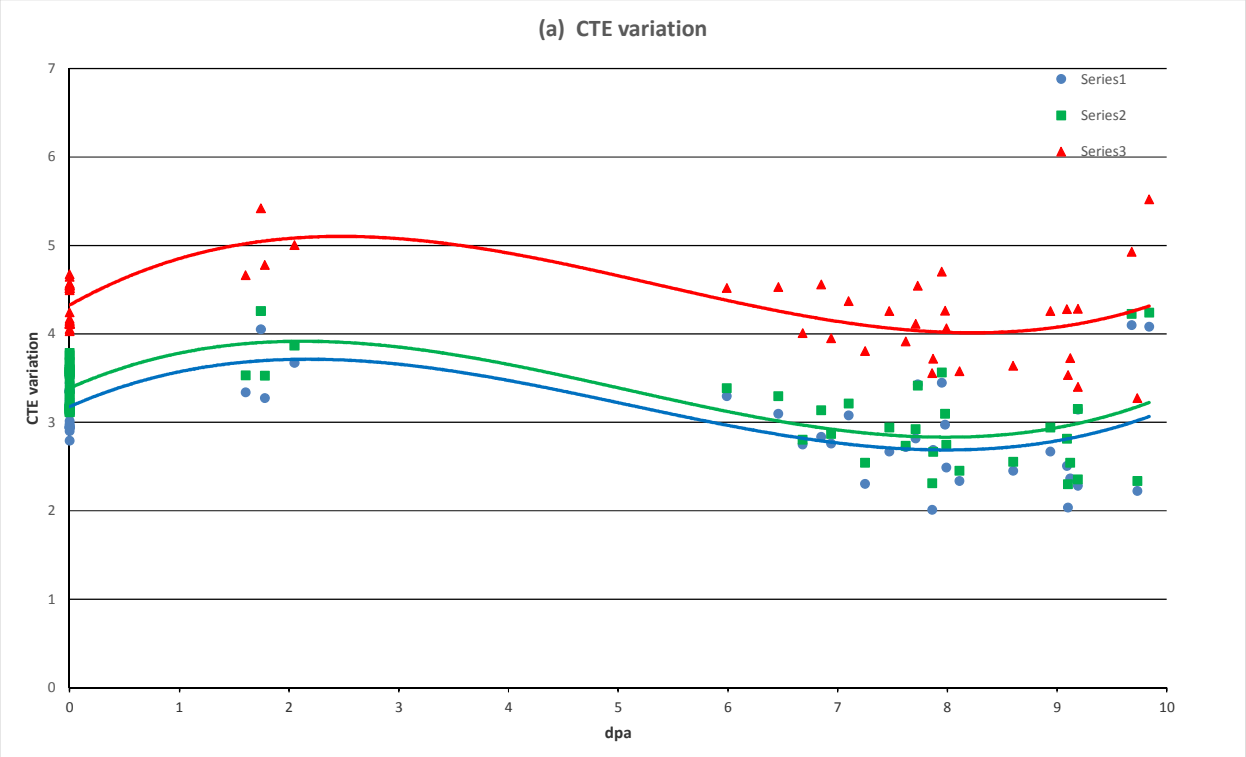

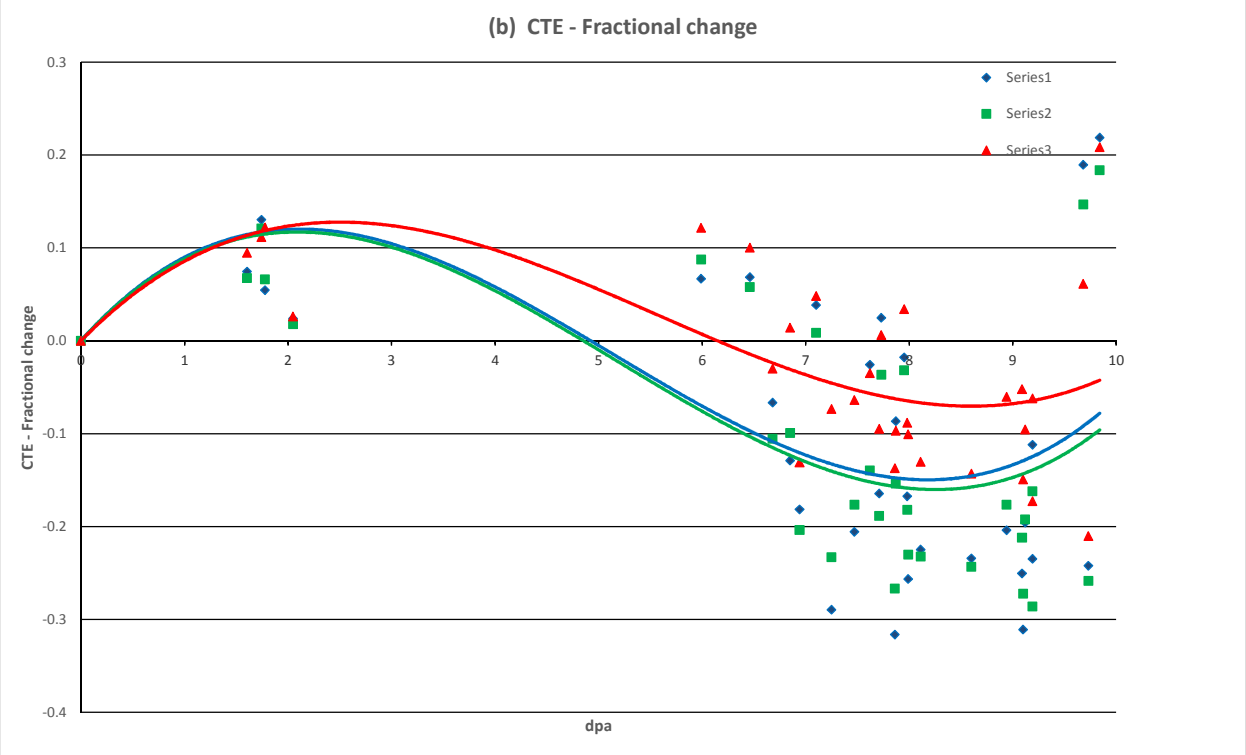

Figure 26- CTE change for IG-430

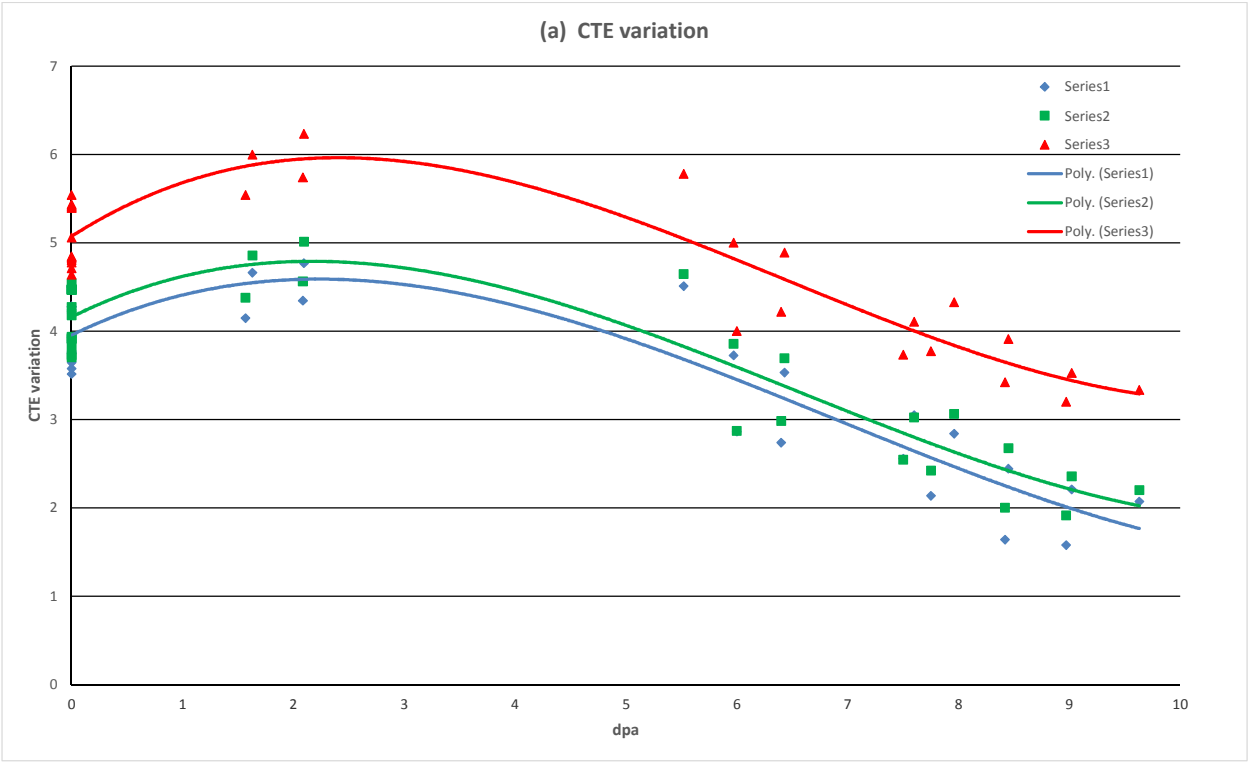

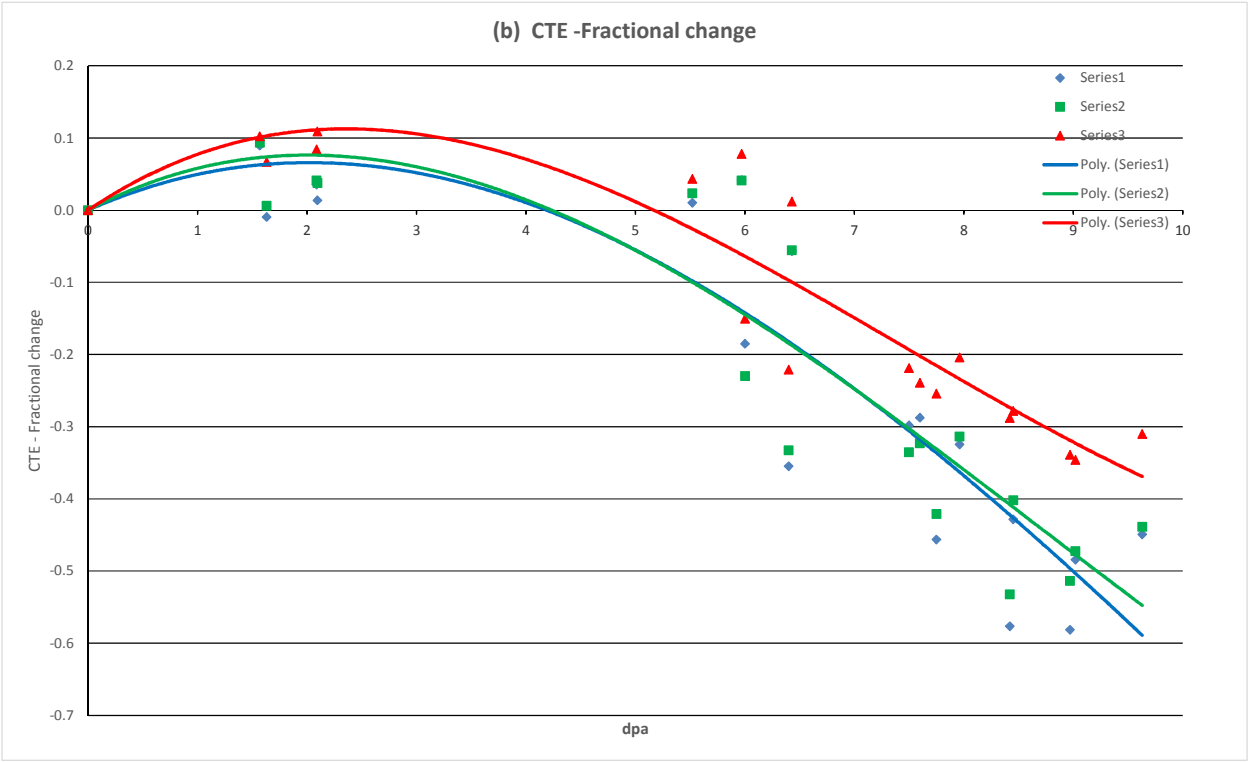

Figure 27 – Thermal conductivity change for NBG-10

(a) Thermal conductivity variation

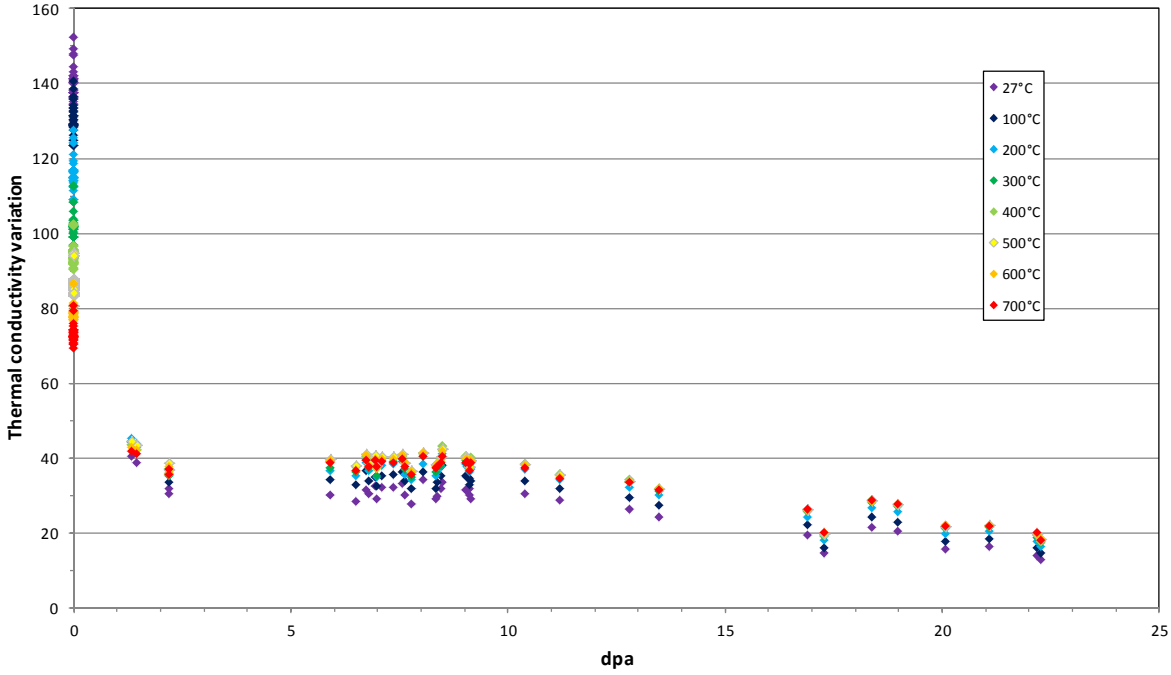

(b) Thermal conductivity - Fractional change

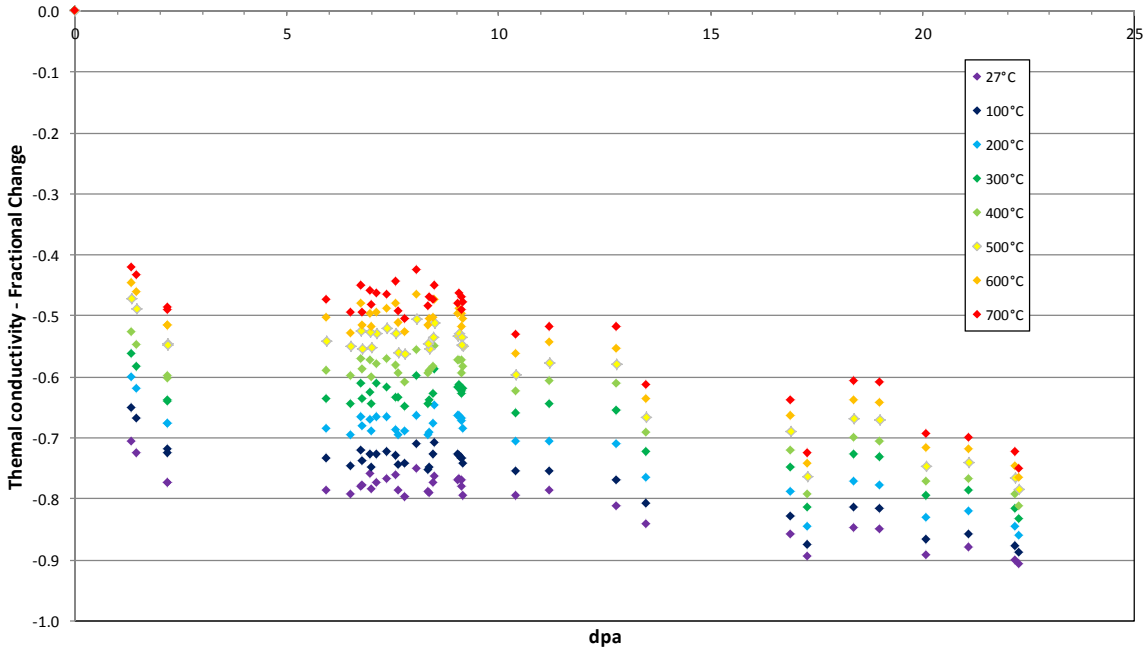

Figure 28 - Thermal conductivity change for NBG-25

(a) Thermal conductivity variation

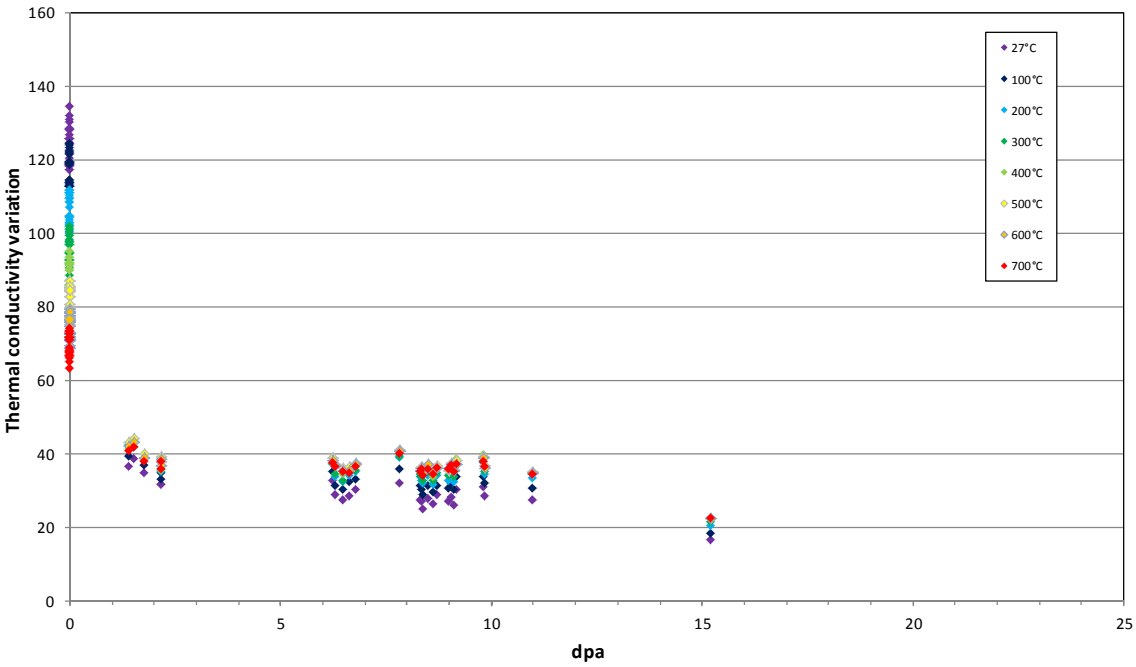

(b) Thermal conductivity - Fractional change

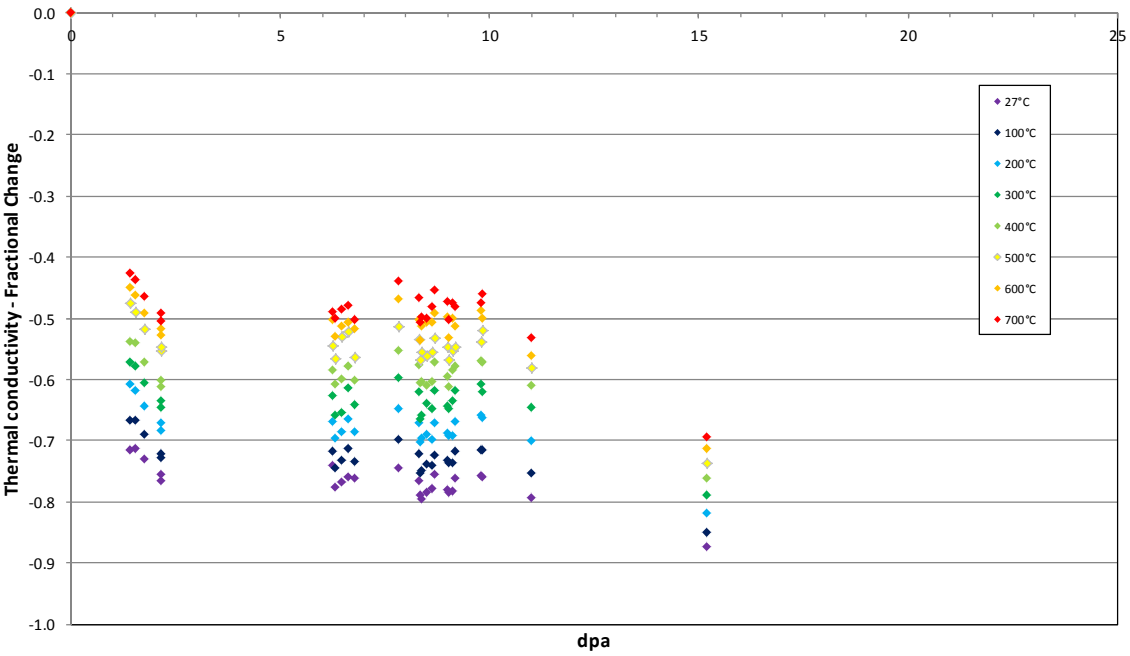

Figure 29- Thermal conductivity change for PCEA

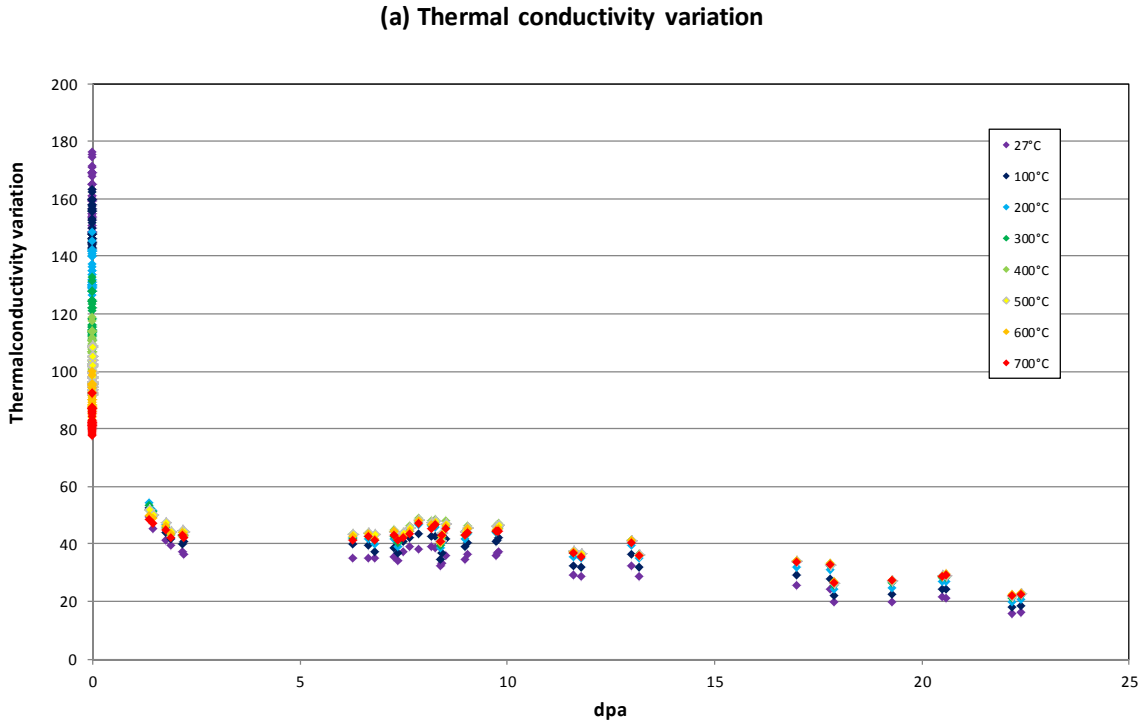

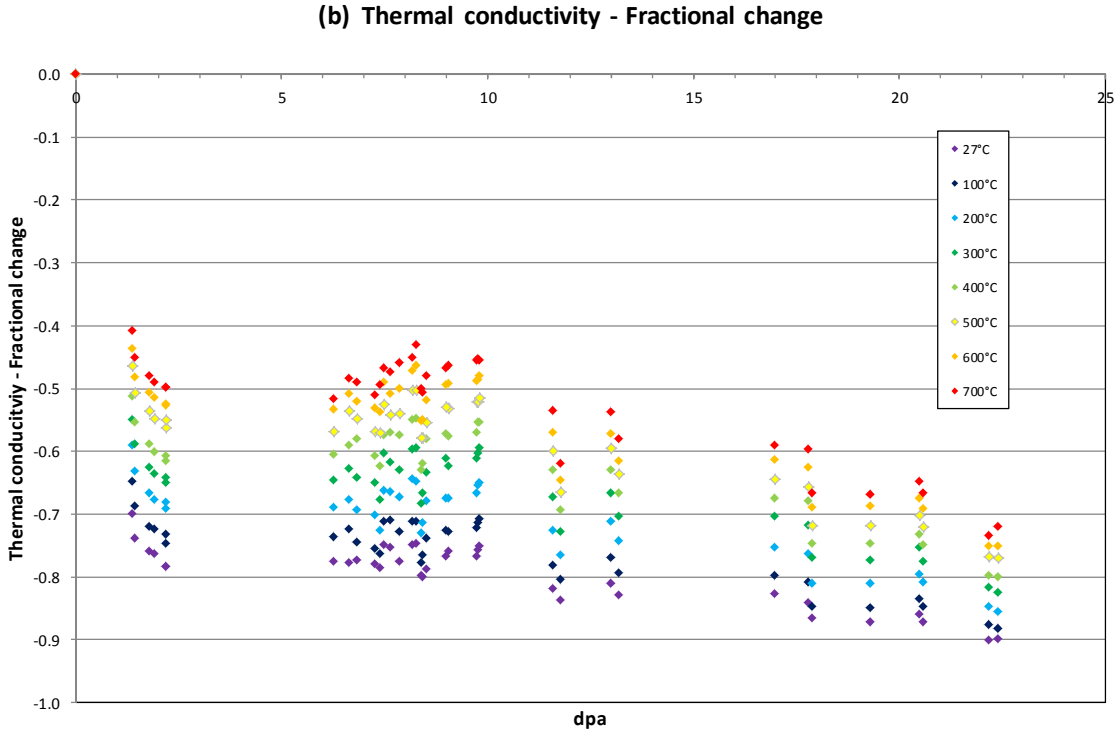

Figure 30- Thermal conductivity change for PPEA

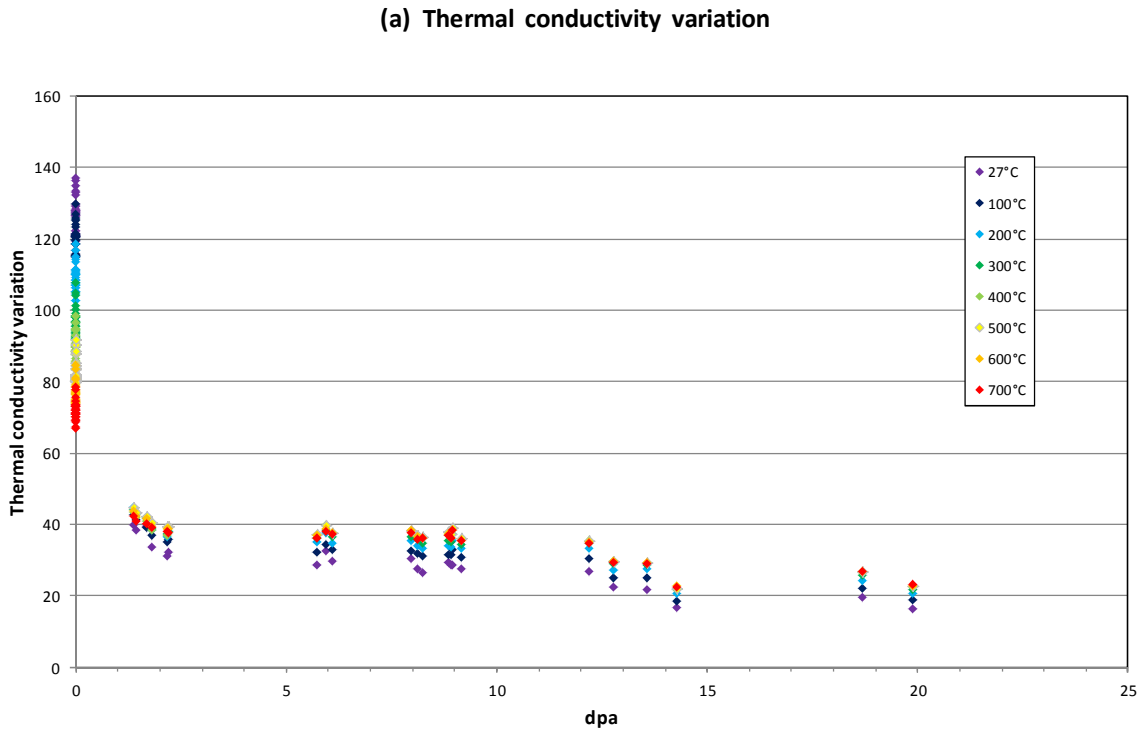

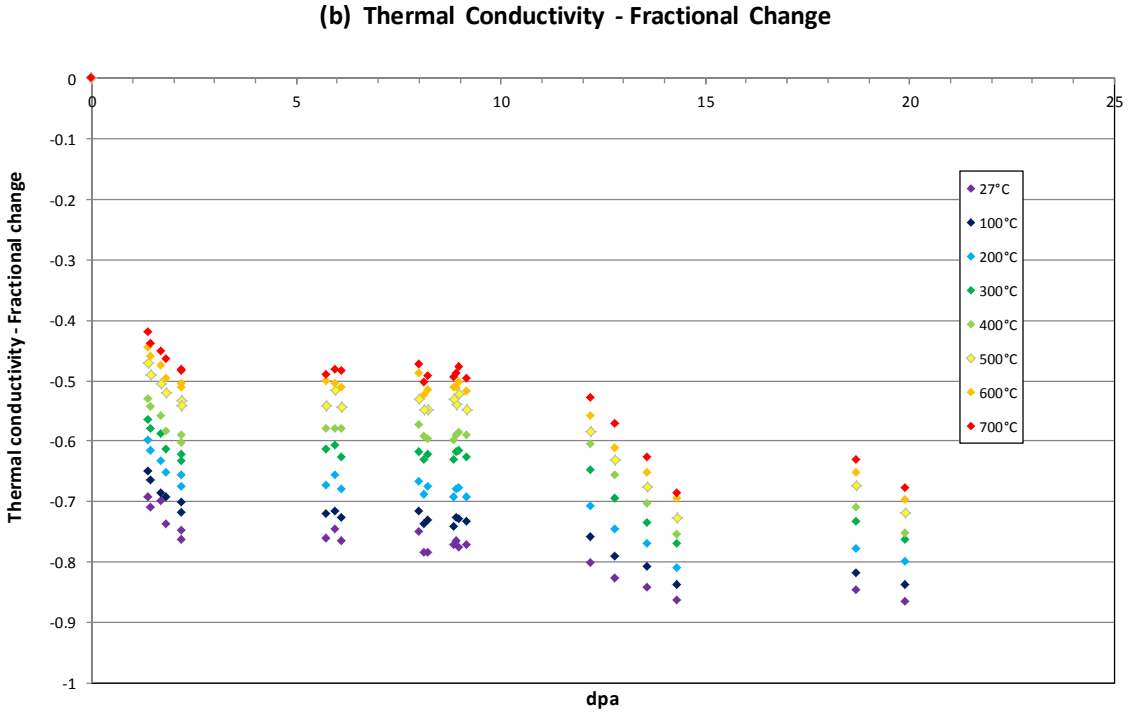

Figure 31- Thermal conductivity change for PCIB

(a) Thermal conductivity variation

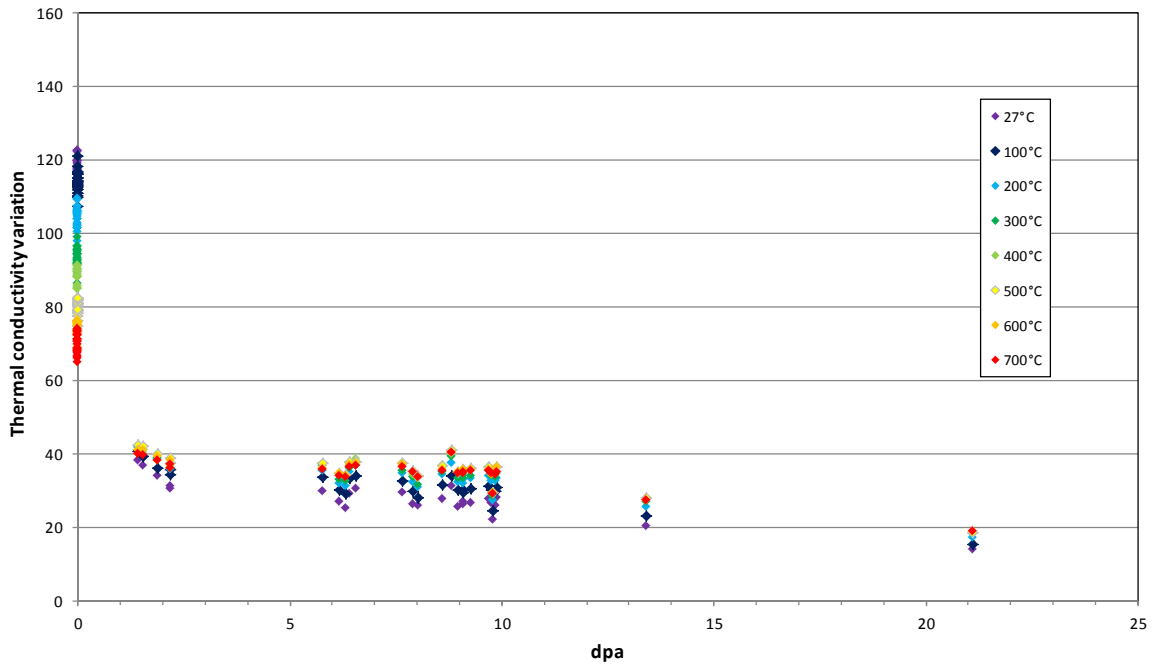

(b) Thermal conductivity - Fractional change

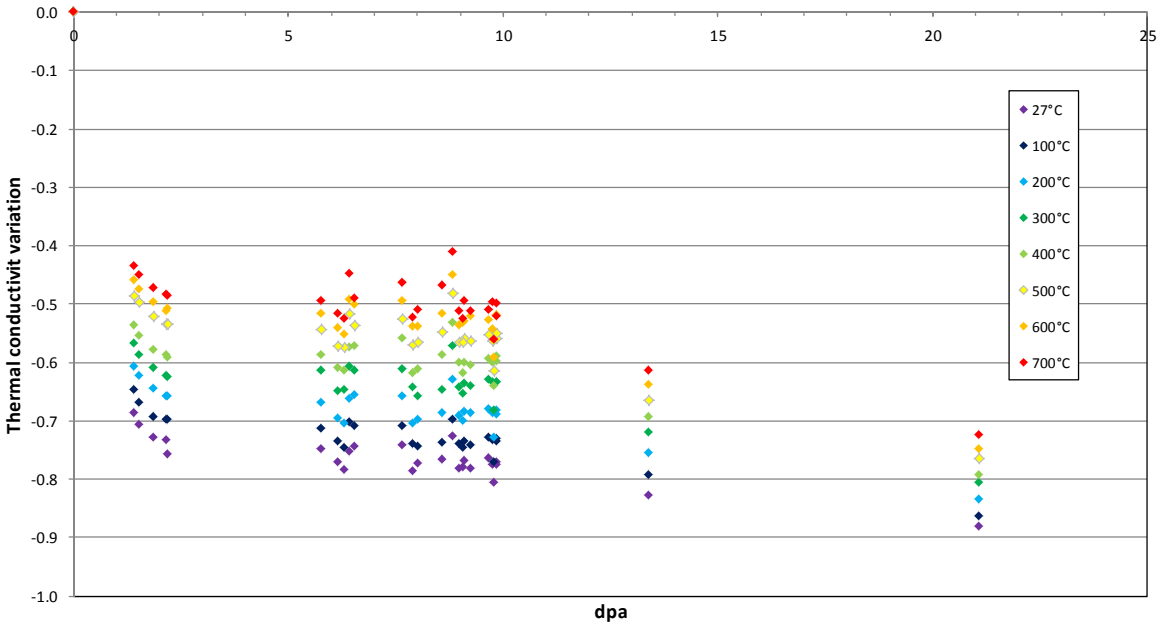

Figure 32- Thermal conductivity change for IG-110

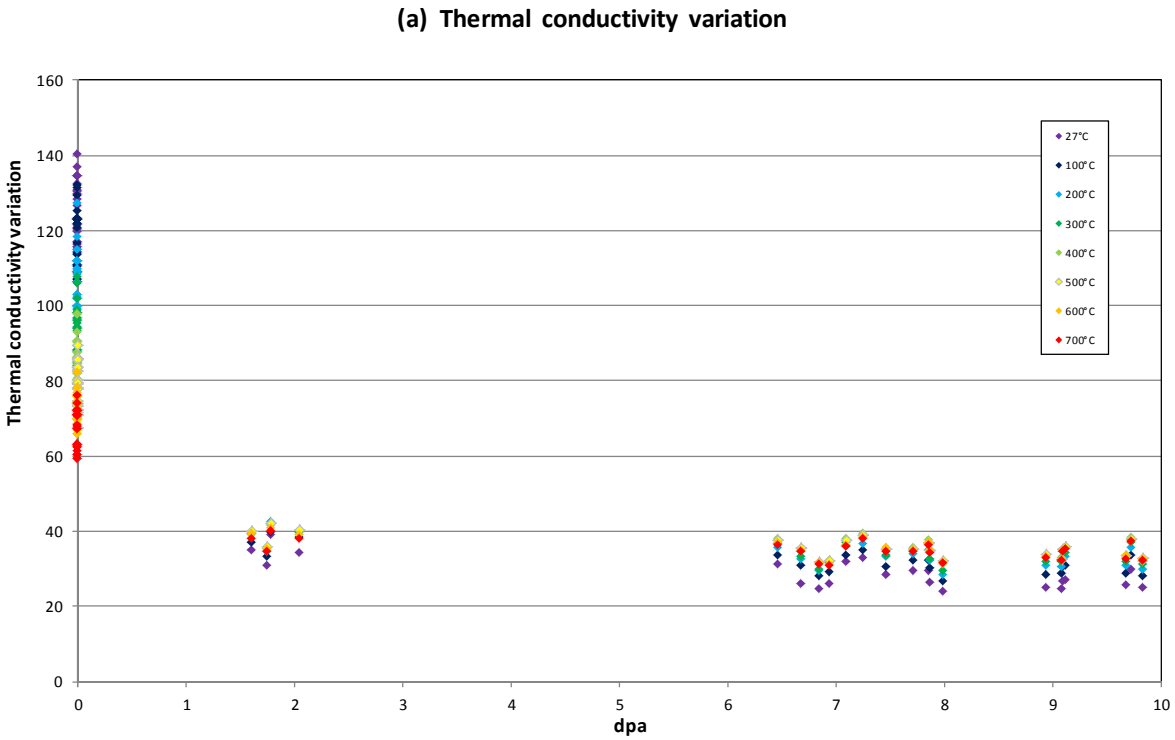

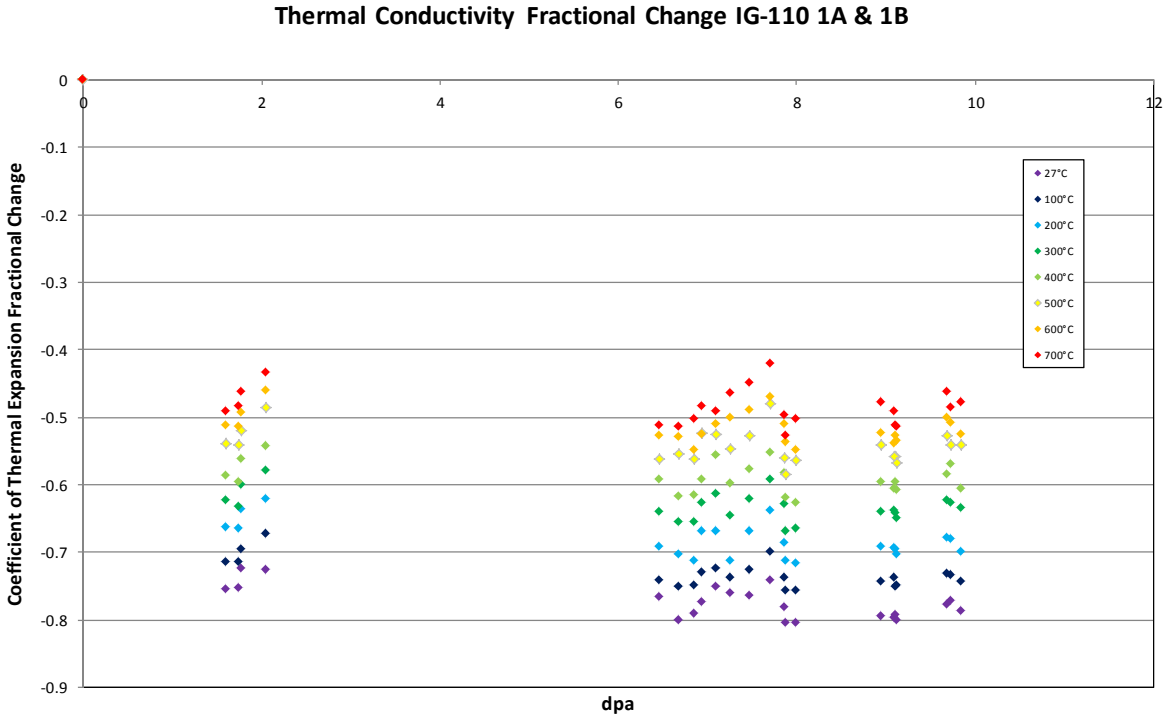

Figure 33- Thermal conductivity change for IG-430